Observatório Nacional

DISSERTAÇÃO DE MESTRADO

COSMOLOGICAL AND PARTICLE PHYSICS IMPLICATIONS OF A NON-MINIMAL RADIATIVE HIGGS INFLATION

RAYFF DE SOUZA

RIO DE JANEIRO
2023

Ministério da Ciência, Tecnologia, Inovações e Comunicações
Observatório Nacional
Programa de Pós-Graduação

Dissertação de Mestrado

COSMOLOGICAL AND PARTICLE PHYSICS IMPLICATIONS OF A NON-MINIMAL RADIATIVE HIGGS INFLATION

por

Rayff de Souza

Dissertação submetida ao Corpo Docente do Programa de Pós-graduação em Astronomia do Observatório Nacional, como parte dos requisitos necessários para a obtenção do Grau de Mestre em Astronomia.

Orientador: Dr. Jailson Alcaniz

Rio de Janeiro, RJ – Brasil
Agosto de 2023

d837 de Souza, Rayff
Cosmological and Particle Physics Implications of a Non-Minimal Radiative Higgs Inflation [Rio de Janeiro] 2023.
xii, 57 p. 29,7 cm: graf. il. tab.

Dissertação (mestrado) - Observatório Nacional - Rio de Janeiro, 2023.

1. Cosmologia. 2. Universo Primordial. 3. Inflação. 4. Bóson de Higgs. I. Observatório Nacional. II. Título.

CDU 000.000.000

"COSMOLOGICAL AND PARTICLE PHYSICS IMPLICATIONS OF A NON-MINIMAL RADIATIVE HIGGS INFLATION"

RAYFF DE SOUZA

DISSERTAÇÃO SUBMETIDA AO CORPO DOCENTE DO PROGRAMA DE PÓS-GRADUAÇÃO EM ASTRONOMIA DO OBSERVATÓRIO NACIONAL COMO PARTE DOS REQUISITOS NECESSÁRIOS PARA A OBTENÇÃO DO GRAU DE MESTRE EM ASTRONOMIA.

Aprovada por:

Dr. Jailson Alcaniz – Observatório Nacional
(Orientador)

Dr. Riccardo Sturani – UNESP

Dr. Júlio Fabris – UFES

Dr. Renato Dupke – Observatório Nacional

RIO DE JANEIRO, RJ – BRASIL
11 DE AGOSTO DE 2023

"And in the end
The love you take
Is equal to the love
You make."
The End - The Beatles

Agradecimentos

Dedico este texto a todos aqueles que se mostraram presentes e, de alguma forma, contribuíram, tanto para minha formação como Mestre em Astronomia, quanto para meu desenvolvimento pessoal ao longo desses dois anos.

Em primeiro lugar, agradeço à minha família, à minha mãe, Sheyla, e ao meu pai, Ewerton, pelo apoio incondicional durante todo esse trajeto, por serem meu alicerce de vida e por sempre me incentivarem na busca pelos meus sonhos. Deixo também minha enorme gratidão ao meu orientador Professor Jailson Alcaniz, por todas as conversas valiosas, não só em relação aos assuntos discutidos no texto, como também sobre Física, Cosmologia e a vida como cientista.

Agradeço às amizades do ON e Casa Branca que tive o prazer de cultivar durante o curso, Bruno, Sousa, Ayslana, Gabriel, Danilo, Ellen, Shao, Thaís, Chris, Giane e os demais. Sem vocês essa jornada teria sido muito mais difícil e guardarei com carinho todos os momentos vividos. Aproveito para desejá-los bastante sucesso no seguimento de suas carreiras. Deixo também meu agradecimento aos meus caros amigos de Natal de longas datas, Dhan, Gustavo, Vitor, Matheus, Rodrigo, Gabriel e Edyan, que sempre estiveram comigo, nos quais deposito minha total confiança e gratidão.

Agradeço aos Professores do CBPF José Helayel e Sebastião Alves Dias por todos os ensinamentos nos cursos que tive o prazer de cursar, além de todo o apoio e diálogos sobre ciência. Agradeço também aos Drs. Jamerson Rodrigues e Micol Benetti, pelas inúmeras interações nesses dois anos e, principalmente, por todo o suporte na elaboração desse texto e do artigo no qual colaboramos juntos. Agradeço aos demais Professores do ON pelos ensinamentos que tanto contribuíram para minha formação. Por fim, agradeço a CAPES pelo suporte e financiamento que possibilitaram a realização desse trabalho.

Rayff de Souza

COSMOLOGICAL AND PARTICLE PHYSICS IMPLICATIONS OF A NON-MINIMAL RADIATIVE HIGGS INFLATION

RESUMO

Neste trabalho, exploramos aspectos de um modelo de Inflação Não-Mínima de Higgs, onde correções radiativas são incluídas a partir da aproximação de Coleman-Weinberg. Por meio de uma análise MCMC, vinculamos o parâmetro que quantifica as correções quânticas ao potencial inflacionário com dados cosmológicos para uma série de valores do número de e-folds da inflação. Além disso, fazemos uma análise geral do período de reaquecimento, a fim de estipular um limite superior para a expansão inflacionária do Universo. A fim de melhor compreender os efeitos do cenário proposto em baixas energias, relacionamos nossos vínculos em cima do parâmetro radiativo com medições de física de partículas na escala eletrofraca, por meio das Equações do Grupo de Renormalização, nos permitindo estimar um limite para a massa do top quark. Por fim, investigamos a quebra da correlação entre a constante de Hubble H_0 e o parâmetro de *clustering* σ_8, o que torna o modelo interessante mediante as tensões cosmológicas discutidas na última década.

Rayff de Souza

COSMOLOGICAL AND PARTICLE PHYSICS IMPLICATIONS OF A NON-MINIMAL RADIATIVE HIGGS INFLATION

ABSTRACT

In this work, we explore aspects of a Non-Minimal Higgs Inflation model, where radiative corrections are included in the Coleman-Weinberg approximation. By means of a MCMC analysis, we constrain the parameter that quantifies the quantum corrections to the potential with cosmological data for a range of the inflationary e-fold number. Also, we perform a general analysis of the reheating stage, in order to estimate an upper limit to the inflationary expansion. In the interest of better understanding the effects of the proposed scenario at low energies, we relate our constraints in the radiative parameter with particle physics measurements at the electroweak scale, via the Renormalization Group Equations, which allows us to estimate a limit to the top quark mass. Finally, we investigate the breaking of the correlation between the Hubble constant H_0 and the clustering parameter σ_8, rendering the model interesting in light of the cosmological tensions discussed in the last decade.

List of Figures

List of Tables

Contents

Introduction

Cosmology is the study of the Universe as a whole, from the smallest to the largest scales of time, space and energy. In 1915, the formulation of the General Theory of Relativity (GR), by Albert Einstein [Einstein, 1915], provided us with an interpretation of the large-scale structure as a dynamic space-time, with its evolution dictated by its matter and energy content. The early thinking of the pioneers of relativistic Cosmology, including Einstein, was that a sensible Universe would look the same everywhere and in all directions, apart from small irregularities in concentrations of stars and planets [Peebles, 2020]. This blossomed into the formulation of the Cosmological Principle, which states that the Universe at cosmological scales should be homogeneous (translational symmetry) and isotropic (rotational symmetry). Early evidences of homogeneity and isotropy already appeared in the 1930s, according to the mapping of galaxy counts in the sky [Hubble, 1934].

In 1922, Alexander Friedmann demonstrated the possibility of an expanding Universe emerging from Einstein's equations [Friedmann, 1922], which was supported by Edwin Hubble's observation of a receding motion of nearby galaxies [Hubble, 1929]. Extrapolating the expansion back in time, we can infer that the current Universe must have evolved from an initial state of extremely high temperature and density, composed of a plasma of different particle species. That marks the beginning of the Hot Big Bang theory.

Throughout the last century, the Big Bang model of the Universe has been constantly supported by cosmological observations. Namely, the predictions for the abundances of light elements produced during Big Bang Nucleosynthesis (BBN), the observation of the near blackbody spectrum of the Cosmic Microwave Background radiation and the distribution of large-scale structure have all been central pillars of Big Bang Cosmology [Baumann, 2022]. However, the theory does not come without its shortcomings.

From the theoretical perspective, the near homogeneity of the Last Scattering Surface (LSS), the flatness of the spatial geometry of the Universe and the absence of unwanted cosmic relics were relentless puzzles of the last century that did not have a dynamical explanation on the basis of the Hot Big Bang. That motivated, in the early 1980s, the proposal of an early period of accelerated expansion, called Cosmological Inflation [Guth, 1981, Starobinsky, 1980]. After this epoch, the Universe would enter the reheating stage, where the known particle species are produced and the standard Big Bang evolution would

follow. However, the nature of the physical entities that might have taken place during inflation and reheating are not yet fully understood. This work attempts to shed some light on the possibilities regarding those scenarios.

On the observational front, the current concordance model of Cosmology, the ΛCDM was established in the early 2000s, after the discovery of the present-day cosmic acceleration [Riess et al., 1998]. Despite being the most successful cosmological model up to date, recent observations have raised important statistical tensions between some of the relevant parameters of the model [Verde et al., 2019].

In parallel to the many developments of Cosmology in the last century, another branch of modern physics was also the stage of some of the most incredible advances of science. The invention of Quantum Field Theory and Gauge Theories allowed for the establishment of the Standard Model of Particle Physics (SM), the most accurate physical theory ever created [Pais, 1986]. Recently, the discovery of the Higgs boson [Chatrchyan et al., 2012], the only scalar particle in the model, marked an important milestone for the SM, while also opening the door for many scientific endeavors for the road ahead.

That said, although this work is primarily concerned with Cosmology, we are interested in developing methods of connecting this branch of science with the study of Elementary Particles. Our method of connecting these areas - among many possibilities - comes from a simple but tempting hypothesis: Could the Standard Model Higgs boson have driven cosmic inflation ? That is a question that has been addressed by many others [Bezrukov and Shaposhnikov, 2008] and is still an active topic of research. The main challenge is, perhaps, satisfying the stringent constraints from both inflationary criteria and low-energy particle physics.

Thus, this work is organized as follows. In Chapter 1 we review the basics of relativistic Cosmology and the paradigm of inflation. In particular, we highlight the scalar field dynamics of the inflationary expansion and how it can be constrained by CMB observations, as well as some general features of the reheating stage. We end by discussing the current concordance model of Cosmology, the ΛCDM, along with its ongoing observational tensions. Chapter 2 is concerned with properties of the Higgs field. First, we discuss the role of the Higgs in the SM, namely the spontaneous symmetry breaking mechanism and the generation of masses for fermions and massive gauge bosons. Then, we focus on recent proposals of elevating the Higgs boson to the status of inflaton, through a non-minimal coupling with gravity. In Chapter 3 we employ the tools developed in the previous Chapters to the non-minimal Higgs inflation with radiative corrections. We motivate the form of the quantum corrections included in the inflationary potential, and analyse how it fits current CMB data. By exploring the reheating stage, we are able to derive an upper limit to the amount of expansion during inflation. Then, we conclude by discussing our two main results. First, we relate our assessment of the radiative corrections to the Higgs potential to the electroweak scale by means of the Renormalization Group Equation, al-

lowing us to estimate an upper limit for the top quark mass. At last, we discuss the results of the MCMC analysis in which a breaking of the correlation between the Hubble constant H_0 and the clustering parameter σ_8, both important parameters of ΛCDM, is found.

Chapter 1

The Standard Model of Cosmology

Among the four fundamental forces of Nature, the one that primarily concerns the field of Cosmology is the gravitational interaction. We have confidence that the Universe is, in average, electrically neutral, so electromagnetism does not play a major role. Since the weak and strong nuclear interactions are short-ranged, that leaves, in principle, gravity to explain all of the dynamics of large-scale structure.

As mentioned, the modern formulation of gravity is based on the General Theory of Relativity of Albert Einstein [Einstein, 1915]. Even though it has passed several tests from within the solar system up to cosmological scales, we know that it is not the final theory of gravity, given that it still lacks a high energy completion, where quantum effects become important. Therefore, GR can be treated as an effective theory for energies below the Planck scale, providing an accurate description of gravity for most of our cosmological purposes. The theory expresses the dynamics of space-time geometry, captured by the metric tensor $g_{\mu\nu}$, in response to its matter and energy content, given by the energy-momentum tensor, $T_{\mu\nu}$. We can represent it mathematically by writing the Einstein-Hilbert action:

$$S = \frac{M_P^2}{2} \int d^4x \sqrt{-g} R \, . \tag{1.1}$$

Here, g is the determinant of the metric tensor, $M_P = (8\pi G)^{-1/2}$ is the reduced Planck mass and R is the Ricci or curvature scalar, which contains up to second order derivatives of the metric. The Einstein equations can be derived by applying the action principle to (1.1):

$$R_{\mu\nu} - \frac{1}{2} R g_{\mu\nu} = M_P^{-2} T_{\mu\nu} \, , \tag{1.2}$$

where the Ricci tensor $R_{\mu\nu}$ is also related to the metric. Cosmology enters the above equation when one proposes an appropriate ansatz for the geometry and energy-momentum content of space-time, which can be done by means of symmetry arguments, i.e. the Cosmological Principle. At large scales ($\gtrsim$ 100 Mpc), the Universe appears to be homogeneous and isotropic, which is consistent with the use of the Friedmann-Lemaitre-

Robertson-Walker (FLRW) metric in the left-hand side of (1.2):

$$ds^2 = g_{\mu\nu}dx^\mu dx^\nu = -dt^2 + a^2(t)\left[\frac{dr^2}{1-kr^2} + r^2(d\theta^2 + \sin^2\theta d\phi^2)\right] . \tag{1.3}$$

Note that the spatial part of the metric is multiplied by an overall scale factor, $a(t)$. The constant k refers to the spatial curvature of the metric, and it assumes the values of $0, 1$ or -1 for a flat, closed and open Universe, respectively.

Accordingly, the right-hand side of (1.2) should also exhibit the properties of homogeneity and isotropy, which is the case if we take the energy-momentum tensor of the Universe to be of the perfect-fluid type:

$$T_{\mu\nu} = (\rho + p)u^\mu u^\nu + p g_{\mu\nu} , \tag{1.4}$$

where ρ, p and u^μ are the fluid's energy density, pressure and four-velocity, respectively.

Therefore, inserting (1.3) and (1.4) into the Einstein equations (1.2), the 00 component yields:

$$H^2(t) = \frac{1}{3M_P^2}\rho(t) - \frac{k}{a^2} . \tag{1.5}$$

Equation (1.5) is called the Friedmann equation, the dynamical equation for the cosmological background. At any given moment in cosmic time, the behaviour of the Universe's expansion rate, captured by the Hubble parameter $H \equiv \frac{\dot{a}}{a}$, is given by the overall energy density of all the combined fluid species in the Universe, $\rho = \sum_i \rho_i$.

The ij components of Einstein equations, combined with the Friedmann equation, yield the acceleration equation, which captures the variation of the expansion rate:

$$\frac{\ddot{a}}{a} = -\frac{1}{6M_P^2}(\rho + 3p) . \tag{1.6}$$

In addition to the Einstein equations, we can impose the general relativistic conservation condition $\nabla_\mu T^{\mu\nu} = 0$, with the ansatz (1.3) and (1.4):

$$\dot{\rho} + 3H(\rho + p) = 0 . \tag{1.7}$$

We have now three equations for the three variables $a(t)$, $\rho(t)$ and $p(t)$. However, only two of them are independent, given that (1.5) was used in the derivation of (1.6). Therefore, in order to close the system of equations, we can use a fluid equation of state, relating its pressure to the energy density:

$$p = w\rho , \tag{1.8}$$

with w being the dimensionless equation of state parameter, which depends on the fluid constituent. For instance, $w_m = 0$ for ordinary and dark matter, $w_r = 1/3$ for radiation and $w_\Lambda = -1$ for a cosmological constant. If one inserts (1.8) into (1.7), we get $\rho \propto a^{-3(1+w)}$.

We can use substitute this result into the Friedmann equation (1.5) in order to find the evolution of the scale factor for a spatially flat Universe dominated by a component with equation of state parameter w:

$$a(t) \propto \begin{cases} t^{\frac{2}{3(1+w)}}, & w \neq -1 \\ e^{Ht}, & w = -1 \, . \end{cases} \tag{1.9}$$

In the interest of estimating the energy density of the various components of the Universe, it is useful to introduce a more natural scale of ρ. This is done by defining the critical density: $\rho_c \equiv 3H^2 M_P^2$, corresponding to the energy density required for the Universe to be spatially flat. Now, for each component, we define the density parameter: $\Omega_i \equiv \frac{\rho_i}{\rho_c} \propto \frac{a^{-3(1+w)}}{\rho_c}$. Thus, we can write the Friedmann equation in terms of Ω_i as

$$H^2(a) = H_0^2 \left[\sum_i \Omega_i a^{-3(1+w_i)} + \Omega_k a^{-2} \right] , \tag{1.10}$$

where the density parameters are now evaluated at the present time.

The above equations form the basis for the dynamical description of the expanding cosmological background. For a Universe composed of ordinary matter and radiation, the pioneers of relativistic Cosmology hoped to be able to fully describe the cosmic past and its future. The issue is that, contrary to what was expected, observations and non-empirical assessments pointed to the existence of exotic components of the cosmos, as well as non-trivial expansion periods.

1.1 The Inflationary Paradigm

As already known in the early days of relativistic Cosmology, a Universe with an initial singularity some finite time in the past, dominated by radiation and matter, has a finite particle horizon. Among other consequences, it means that a light signal could only have traveled so far from the singularity to a given moment in cosmic history, and this maximum distance defines the causal horizon of a given observer. As discussed previously, current large-scale observations are consistent with the picture of a Universe which was highly homogeneous and isotropic at initial times. It turns out that, on the basis of the causal structure of standard FLRW Cosmology, the primordial Universe was composed of at least $\sim 10^{83}$ causally disconnected regions [Guth, 1981], which could not have established causal contact and hence could not have attained thermal equilibrium. Therefore, the puzzle of a highly homogeneous early Universe is called the horizon problem of standard Big Bang Cosmology.

Our modern understanding of this issue is most commonly addressed in terms of the

near homogeneity of the CMB. The maximum distance that an observer can establish causal contact at a given time in an expanding Universe is given by the comoving Hubble scale[1] $(aH)^{-1}$. The comoving particle horizon is obtained by the logarithmic integration of this quantity throughout cosmic history [Baumann, 2022]:

$$d_h(\eta) = \int_{\ln a_i}^{\ln a} (aH)^{-1} d\ln a \ , \tag{1.11}$$

with η being the conformal time coordinate, related to the cosmic time according to $d\eta = \frac{dt}{a(t)}$. In standard FLRW Cosmology, the integral (1.11) is dominated by contributions of $(aH)^{-1}$ from late times, so that the particle horizon is approximately the same as the Hubble horizon.

It is important to distinguish between the causal interpretation of the comoving Hubble radius $(aH)^{-1}$ and the comoving particle horizon d_h. If regions are separated by distances greater than the comoving Hubble scale, they cannot be on causal contact *now*[2]. However, if they are separated by distances greater than the particle horizon, then they could have *never* communicated with one another. In standard FLRW Cosmology, $(aH)^{-1}$ is a monotonically increasing function, so that regions entering causal contact right now could have never communicated with each other in the past. In fact, we see patches of the CMB distribution, separated on scales larger than each others Hubble horizon, that display near thermal equilibrium. Therefore, these regions could not have been at causal contact during last-scattering, or at any past time. Also, these scales appear to be correlated, as measured in the statistical properties of the CMB temperature anisotropies. Thus, the horizon problem can be comprehended as an interplay between the concepts of the Hubble and particle horizons.

In addition, it appeared in 1970 that the overall energy density of the Universe was very close to the critical density [Hawking and Israel, 2010], which implied that our spatial geometry is approximately flat. The issue with this conjecture is that an $|\Omega_k|$ very close to zero implies an initial curvature parameter fine-tuned to several orders of magnitude, since $|\Omega_k|$ is a monotonically increasing function in standard Big Bang Cosmology. Therefore, basically any deviation from $|\Omega_k| = 0$ would produce a larger present-day curvature. This is called the flatness problem and, together with the horizon problem[3], produced serious doubts regarding the predictive character of the Big Bang theory.

A solution was put forth in the early 1980s, by Alan Guth [Guth, 1981] and Alexei Starobinsky [Starobinsky, 1980], independently. In light of the causality issues arising from the growing character of the comoving Hubble sphere in standard FLRW Cosmol-

[1] Often called (comoving) Hubble radius or (comoving) Hubble horizon.

[2] Specifically, particles outside of the comoving Hubble sphere cannot make causal contact during a characteristic expansion time H^{-1}.

[3] The absence of magnetic monopoles and other relics are together called the monopole problem by some authors [Baumann, 2012].

ogy, one can stipulate a period of a *decreasing* Hubble radius prior to the Hot Big Bang, called Cosmological Inflation[4]. Accordingly, we can impose that regions that are outside of the Hubble horizon in the CMB at last-scattering, were in fact inside the horizon at some point during inflation, in which they had time to establish causal contact and achieve thermal equilibrium. These scales leave the shrinking Hubble sphere during inflation, only to re-enter the growing horizon at later times, during standard FLRW evolution. A schematic picture of this mechanism is depicted in Figure 1.1.

Since the particle horizon d_h is the logarithmic integral of the comoving Hubble radius

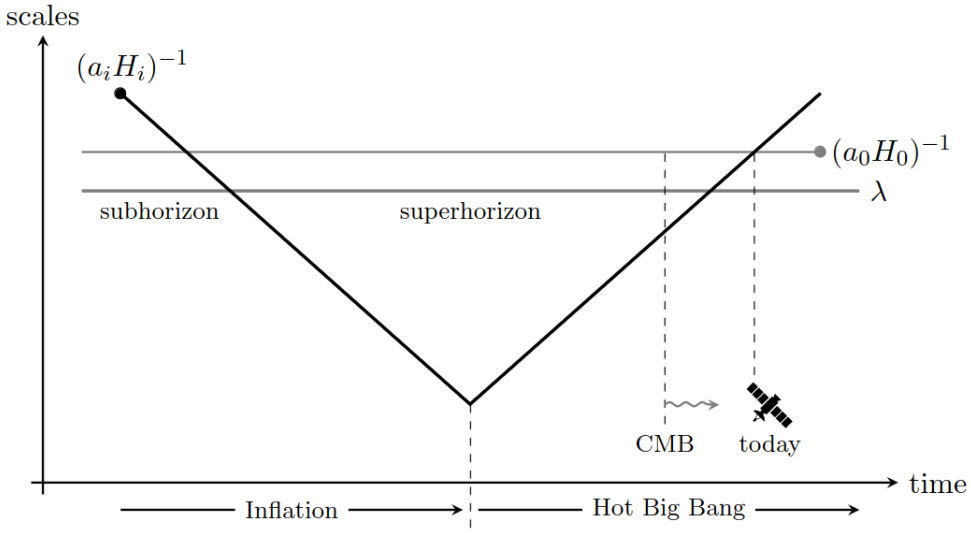

Figure 1.1: Illustration of the way inflation solves the problem of superhorizon correlations. One can see that a given perturbation with characteristic wavelength λ was outside the horizon at the moment of CMB decoupling, but was inside the horizon at some point during inflation [Baumann, 2022].

- see (1.11) - the particle horizon continues to grow during inflation, despite a decreasing $(aH)^{-1}$. Therefore, the inflationary expansion is a mechanism of making the particle horizon much larger than the comoving Hubble scale, so that regions cannot communicate today but were in causal contact early on, contrary to what was predicted by the Hot Big Bang.

The flatness problem can also be conveniently solved in inflation as a consequence of a shrinking Hubble sphere. Since the curvature parameter is written as $|\Omega_k| = \frac{1}{(aH)^2}$, it is driven to zero during the inflationary expansion, so that $|\Omega_k| = 0$ is an attractor independently of its initial value. Even considering the growth of Ω_k in the standard FLRW evolution, if inflation lasts long enough, we can safely satisfy Planck's constraints of $|\Omega_k| < 0.005$ [Aghanim et al., 2020a].

Inflation is most commonly - and equivalently - defined as a period of accelerated

[4]Following the reasoning of [Baumann, 2022], we prefer to use a period of a shrinking Hubble sphere as the very definition of inflation, since it relates more directly to the horizon problem and the generation of correlated cosmological fluctuations.

expansion in the very early Universe. One can see that it follows directly from the requirement of a decreasing Hubble radius:

$$\begin{aligned} &\frac{d}{dt}(aH)^{-1} = \frac{d}{dt}\dot{a}^{-1} = -\frac{\ddot{a}}{\dot{a}^2}, \\ &\frac{d}{dt}(aH)^{-1} < 0 \implies \ddot{a} > 0 \,. \end{aligned} \tag{1.12}$$

Although spacetime expands rapidly during inflation, all physical quantities are said to be slowly varying. One can see this by rewriting expression (1.12) as

$$\begin{aligned} \frac{d}{dt}(aH)^{-1} = -\frac{\dot{a}H + \dot{H}a}{(aH)^2} = -\frac{1}{a}(1-\varepsilon), \\ \varepsilon \equiv -\frac{\dot{H}}{H^2} \,, \end{aligned} \tag{1.13}$$

where ε is called the slow-roll parameter. Thus, we see that a decreasing Hubble radius $\partial_t(aH)^{-1} < 0$ is associated with $\varepsilon < 1$. If we take the limit in which $\varepsilon \to 0$, we find that

$$\begin{aligned} \varepsilon \to 0 &\implies \dot{H} \approx 0 \\ &\implies H \approx \text{const} \\ &\implies a(t) \propto e^{Ht} \,. \end{aligned} \tag{1.14}$$

Thus, inflation is usually formulated as an expansion around a quasi-de Sitter spacetime, in which the Hubble parameter is almost constant (slowly varying) and the expansion is quasi-exponential[5]. From (1.9), we can see that the exponential expansion is associated with a dominant component with $w = -1$.

One can wonder how much inflation is needed in order to solve the horizon and flatness problems. Of course, as mentioned, we at least require that the largest observed scales on the CMB were inside the Hubble horizon at some point during inflation. A more general way to estimate the duration of the inflationary expansion is to require the whole observable Universe (the comoving Hubble sphere today) to be smaller than the Hubble horizon at the beginning of inflation:

$$(a_0 H_0)^{-1} < (a_i H_i)^{-1} \,. \tag{1.15}$$

Since the Hubble parameter stays approximately constant during inflation, $H_i \approx H_{end}$, the amount by which the comoving Hubble radius decreases is equal to the amount by which the scale factor increases. Therefore, we can quantify the inflationary expansion

[5] One cannot set $\varepsilon = 0$ because inflation has to end some time, so the expansion cannot be exactly de Sitter.

according to the number of e-folds:

$$N_{inf} \equiv \ln \frac{a_{end}}{a_i} \, . \tag{1.16}$$

The total number of e-folds depends on the energy scale of inflation and details about the reheating process, which marks the transition between inflation and the Hot Big Bang (see Section 1.1.3).

1.1.1 The Slow-Roll Mechanism

For the purpose of further investigating the dynamics of the inflationary expansion, we have to specify the dominant component of the Universe during inflation, which sources the evolution of the quasi-de Sitter background. Perhaps the simplest proposal to achieve an expansion of such type is to consider the existence of a scalar field $\phi(t, \mathbf{x})$ in the early Universe, called the inflaton. The general action for a scalar field in curved spacetime is given by:

$$S = \int d^4x\sqrt{-g}\left[\frac{M_P^2}{2}R - \frac{1}{2}\partial_\mu\phi\partial^\mu\phi - V(\phi)\right] \, , \tag{1.17}$$

where the second and third terms are the inflaton's kinetic and potential energy, respectively. To check weather a field of such type can give rise to an inflationary Universe, we assume a fluid interpretation of the field condensate. This can be done by obtaining the energy-momentum tensor $T_{\mu\nu}$ for the inflaton fluid. Under a variation of (1.17) with respect to the inverse metric, the action changes as

$$\begin{aligned} \delta S &= -\frac{1}{2}\int d^4x\sqrt{-g}T_{\mu\nu}\delta g^{\mu\nu} \\ T_{\mu\nu} &= \partial_\mu\phi\partial_\nu\phi - g_{\mu\nu}\left(\frac{1}{2}\partial_\alpha\phi\partial^\alpha\phi + V(\phi)\right) \, . \end{aligned} \tag{1.18}$$

Comparing with (1.4), we find that the energy density and pressure, as well as the equation of state parameter, for the inflaton are:

$$\begin{aligned} \rho &= \frac{1}{2}\dot{\phi}^2 + V(\phi) \\ p &= \frac{1}{2}\dot{\phi}^2 - V(\phi) \\ w &= \frac{p}{\rho} = \frac{\frac{1}{2}\dot{\phi}^2 - V(\phi)}{\frac{1}{2}\dot{\phi}^2 + V(\phi)} \, . \end{aligned} \tag{1.19}$$

The condition $w = -1$ can be satisfied if the inflaton's potential energy dominates over its kinetic energy. Therefore, by making $V(\phi) \gg \frac{1}{2}\dot{\phi}^2$ in (1.19) we obtain $w \approx -1$, which causes the cosmic background to accelerate while dominated by ϕ.

The set of dynamical equations for the inflationary background are the Friedmann equation (1.5) with ρ given by (1.19) and the Klein-Gordon equation, derived by conservation of the energy-momentum tensor, $\nabla_\mu T^{\mu\nu} = 0$. Therefore, we arrive at:

$$H^2 = \frac{1}{3M_P^2}\left[\frac{1}{2}\dot{\phi}^2 + V(\phi)\right] , \tag{1.20}$$

$$\ddot{\phi} + 3H\dot{\phi} + V'(\phi) = 0 . \tag{1.21}$$

These are coupled equations. The scalar field behavior dictates the evolution of the Hubble rate, which in turn induces a friction in the inflationary background. We would like to investigate the conditions that give rise to slow-roll inflation in this scenario.

Combining (1.20) and (1.21) to get $\dot{H} = -\frac{1}{2}\frac{\dot{\phi}^2}{M_P^2}$, and using the condition of dominant potential energy, we can express the slow-roll parameter as

$$\varepsilon \equiv -\frac{\dot{H}}{H^2} = \frac{\frac{3}{2}\dot{\phi}^2}{\frac{1}{2}\dot{\phi}^2 + V(\phi)} , \tag{1.22}$$

where in the last equality, the denominator comes from (1.20). We can see that the condition of a flat potential, i.e $V(\phi) \gg \dot{\phi}$ is equivalent to $\varepsilon \ll 1$. Hence, the slow-roll condition is satisfied if inflation happens via scalar field that slowly rolls down its approximately flat potential.

In order for slow-roll inflation to persist, the acceleration of the field must also be small. It is useful to define the dimensionless parameter $\delta \equiv -\frac{\ddot{\phi}}{H\dot{\phi}}$. The condition $\delta \ll 1$ is equivalent to stating that $\ddot{\phi} \ll 3H\dot{\phi}$ in (1.21), which assures that the inflaton's kinetic energy stays subdominant during inflation. Under the assumptions $\{\varepsilon, |\delta|\} \ll 1$, the inflationary background equations are simplified to:

$$H^2 \approx \frac{V}{3M_P^2} , \tag{1.23}$$

$$\dot{\phi} \approx \frac{V'}{3H} . \tag{1.24}$$

Now, taking the time derivative of (1.24), we obtain $3\dot{H}\dot{\phi} + 3H\ddot{\phi} \approx -V''\dot{\phi}$ which we can use to introduce a new parameter η defined by:

$$\eta \equiv \varepsilon + \delta = -\frac{\ddot{\phi}}{H\dot{\phi}} - \frac{\dot{H}}{H^2} = \frac{V''}{3H^2} . \tag{1.25}$$

Substituting (1.23) and (1.24) in (1.22) and (1.25), we arrive at the slow-roll parameter expressed exclusively in terms of the inflaton potential[6]:

$$\begin{aligned} \varepsilon &= \frac{M_P^2}{2}\left(\frac{V'}{V}\right)^2 \\ \eta &= M_P^2\frac{V''}{V} \ . \end{aligned} \tag{1.26}$$

The parameters (1.26) are extremely useful to judge weather a scalar potential $V(\phi)$ can give rise to slow-roll inflation, i.e if it allows for a regime where $\{\varepsilon, |\eta|\} \ll 1$. They are important for constraining inflationary models with data and we will come back to them in the next Chapters.

As far as the inflationary number of e-folds, we can rewrite expression (1.16) in terms of the inflaton's evolution:

$$N_{inf} \equiv \ln\frac{a_{end}}{a_i} = \int_{t_i}^{t_{end}} H dt = \int_{\phi_i}^{\phi_{end}} \frac{H}{\dot{\phi}} d\phi \approx \frac{1}{M_P^2}\int_{\phi_i}^{\phi_{end}} \frac{V}{V'} d\phi \ . \tag{1.27}$$

As we can see from Figure 1.1, we require the amount of expansion from the moment a given wavelength λ leaves the horizon to the end of inflation, to be equal to the expansion from the end of inflation until today. The first quantity is precisely the above expression for N_{inf} evaluated between field values ϕ_*, associated with the moment λ crosses the horizon, and ϕ_{end}, which marks the end of the inflationary period. For a wavenumber k representative of a given scale λ, we define the e-fold number from horizon crossing up to the end of inflation as

$$N_k = \frac{1}{M_P^2}\int_{\phi_*}^{\phi_{end}} \frac{V}{V'} d\phi \ . \tag{1.28}$$

The relevant scales probed by CMB and LSS observations seem to correspond to a range of e-folds between 50-60 [Liddle and Leach, 2003], assuming a reference scale of $k = 0.05$ Mpc^{-1}, which will guide our exploration of N_k in Chapter 3.

1.1.2 Contact with Observations

The signatures of cosmological inflation are most generally inferred from observations of the statistical nature of the CMB and large-scale structure. Although the detection of a sea of thermal background radiation was extremely important for the establishment of the Hot Big Bang in the 1960s [Peebles, 2020], the main observational advances in Cosmology are now tied to the study of small perturbations around the homogeneous background. Therefore, the analysis of cosmological perturbations involves the treatment of fluctuations of the metric and the energy momentum-tensor, as they are related through the Einstein (1.2) and conservation (1.7) equations evaluated up to linear order in perturbation theory.

[6] From now on, we will denote the parameters (1.26) collectively as the slow-roll parameters.

Our current theoretical understanding of how those perturbations were generated is intimately tied with the development of inflationary cosmology in the 1980s. The theory, initiated by Mukhanov and Chibisov [Mukhanov and Chibisov, 1981] is based on zero-point quantum fluctuations of inflaton perturbations around the classical background. In the usual setting, the perturbations of the inflaton can effectively be treated as a scalar field in a classical curved background[7]. The quantization of those perturbations closely follows the standard treatment of a quantum harmonic oscillator if the fluctuations happen deep enough in the inflationary regime, where all relevant scales are well inside the horizon [Baumann, 2012, Birrell and Davies, 1984].

In GR, due to our freedom of choosing coordinates which leave the line element ds^2 invariant, we often specify the coordinate system in order to perform calculations, which is equivalent to choosing a *gauge*. Therefore, in the *spatially flat gauge*, the computation of the variance of inflaton perturbations with characteristic wavenumber k reads

$$\langle \delta\phi_k \delta\phi_{k'} \rangle = (2\pi^3)\delta(\mathbf{k}+\mathbf{k}')\frac{H^2}{2k^3} \, . \tag{1.29}$$

Although this variance offers a direct link to quantum zero-point fluctuations of the inflaton, the statistics of primordial cosmological perturbations are most commonly expressed in terms of the comoving curvature perturbation $\mathcal{R}$. In the spatially flat gauge, it is related to the inflaton perturbations according to $\mathcal{R} = H\frac{\delta\phi}{\dot{\phi}}$. One can show that $\mathcal{R}$ stays constant outside the horizon, so that it suffices to compute its variance at the moment of horizon crossing. Using (1.29), we calculate the variance of the comoving curvature perturbation as

$$\begin{aligned} \langle \mathcal{R}_k \mathcal{R}_{k'} \rangle &= \left(\frac{H}{\dot{\phi}}\right)^2 \langle \delta\phi_k \delta\phi_{k'} \rangle = (2\pi)^3 \delta(\mathbf{k}+\mathbf{k}')\frac{H_*^2}{2k^3}\frac{H_*^2}{\dot{\phi}_*^2} \\ &= (2\pi)^3 \delta(\mathbf{k}+\mathbf{k}')\mathcal{P}_{\mathcal{R}}(k) \, , \end{aligned} \tag{1.30}$$

where $\mathcal{P}_{\mathcal{R}}(k)$ is called the power spectrum of comoving curvature perturbations. It is the Fourier transform of the two-point correlation function $\xi(r)$, which is associated with the probability of finding two correlated elements separated by a distance r in a distribution sample. Thus, $\mathcal{P}_{\mathcal{R}}(k)$ contains the statistical information of primordial perturbations in the large-scale structure[8]. Therefore, the primordial power spectrum serves as an input of initial conditions for the propagation of perturbations as cosmic sound waves in the primordial plasma, which leave striking signatures in the CMB temperature distribution.

[7] In the following we assume a light scalar field ($m_\phi \ll H$).

[8] In standard single field slow-roll inflation, the variance of $\delta\phi$ is computed from the quantization of an approximately free harmonic oscillator, which has a Gaussian distribution in real space. Therefore, the two-point function (or power spectrum) contains all the statistical information and higher-order correlations vanish. More involved inflationary models, such as multi-field inflation, predict the existence of non-gaussianities, which would be detected as higher point correlations in the CMB anisotropies.

In the literature, it is customary to use the dimensionless power spectrum $\Delta^2_{\mathcal{R}}(k) = \frac{k^3}{2\pi^2}\mathcal{P}_{\mathcal{R}}(k)$, which, according to (1.30), is written as

$$\Delta^2_{\mathcal{R}}(k) = \frac{H_*^2}{(2\pi)^2}\frac{H_*^2}{\dot{\phi}_*^2} = \frac{1}{8\pi^2 M_P^2}\frac{H_*^2}{\varepsilon_*}\,, \tag{1.31}$$

where, in the last equality, we have substituted the definition of the slow-roll parameter ε. If the inflationary expansion was exactly de Sitter, one would expect a perfect scale invariance of the dimensionless power spectrum (1.31). But since inflation has to end, the expansion rate is not exactly constant, and scales exit the horizon at slightly different values of H_*. Therefore, we can parameterize $\Delta^2_{\mathcal{R}}(k)$ according to:

$$\begin{aligned}
\Delta^2_{\mathcal{R}}(k) &= A_S\left(\frac{k}{k_*}\right)^{n_S-1}\,,\\
A_S &\equiv \frac{1}{8\pi^2 M_P^2}\frac{H_*^2}{\varepsilon_*},\\
n_S - 1 &\equiv \frac{d\ln\Delta^2_{\mathcal{R}}(k)}{d\ln k}\,.
\end{aligned} \tag{1.32}$$

The quantities A_S and n_S are denoted the amplitude of primordial scalar perturbations and the scalar spectral index, respectively. The scale k_* is taken as a reference point, and all quantities on the right-hand side are evaluated at the moment k_* crosses the horizon.

As mentioned, single field slow-roll inflation predicts a percent-level deviation from perfect scale invariance ($n_S = 1$). A_S and n_S can be constrained, as well as the other parameters of a given cosmological model, by adjusting the theoretical curve with the observed CMB power spectrum in Figure 1.2.

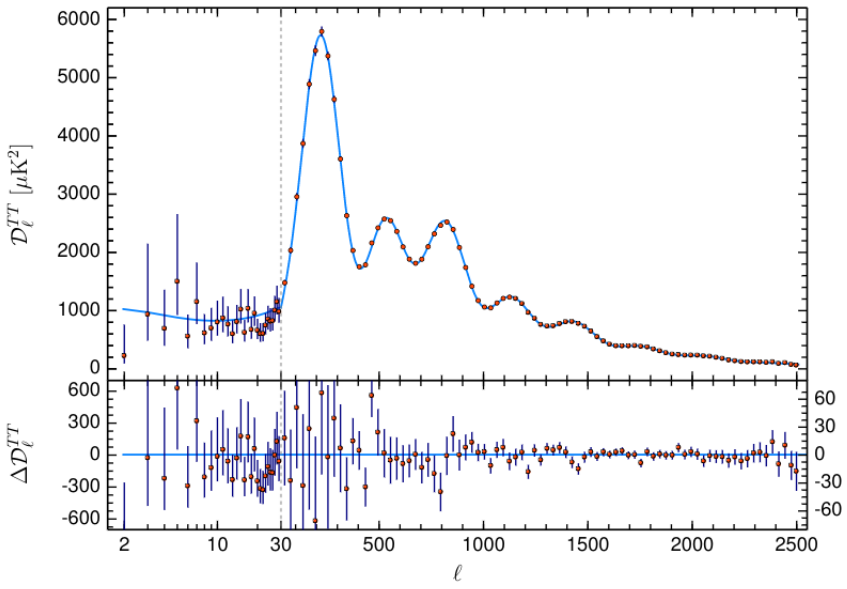

Figure 1.2: The CMB temperature power spectrum [Aghanim et al., 2020a].

The horizontal axis in Figure 1.2 are Legendre multipoles, which appear as a result of the two-dimensional projection of the CMB temperature distribution in the sky in terms of spherical harmonics. The main contribution to the power at a given multipole comes from scales $k \sim \frac{l}{\chi_*}$, where χ_* is the conformal distance to the last-scattering surface. The location of the peaks in the power spectrum are associated with the k modes that entered the horizon and sourced cosmic sound waves in the primordial plasma that were at an extreme of an oscillation at the moment of CMB decoupling[9]. Thus, these oscillations were captured in the LSS as correlations at those particular scales. The locations of the peaks are at $l_{\text{peaks}} \sim n\pi\frac{d_A}{r_s}$, which depend on the physics of the oscillatory motion of the photon-baryon fluid, associated with the sound horizon at recombination r_s, and on the angular distance to the last scattering surface d_A. Naturally, these physical quantities are sensitive to the adopted cosmological model and its parameters. Also, the correlations in the CMB anisotropies indicate that the initial perturbations are strongly adiabatic, where the initial departure from homogeneity of different species is determined by a single degree of freedom [Lyth and Liddle, 2009]. In what concerns the primordial power spectrum, a change of A_S produces an overall scaling of the total spectrum, while n_S influences the relative power of large to smaller scales. The latest constraints from CMB data yield $A_S \sim 2.1 \cdot 10^{-9}$ and $n_S \sim 0.9603$ [Aghanim et al., 2020a], which is a remarkable agreement with the inflationary picture.

Apart from scalar fluctuations, the metric exhibits tensor perturbations, which are also sourced from the dynamics of the inflationary period. By splitting the metric tensor into a homogeneous background and a perturbation h_{ij}, we can perform a similar quantization of the two tensor polarization modes, as was done for the scalar case. The resulting dimensionless power spectrum of tensor perturbations reads [Baumann, 2012]

$$\Delta_t^2(k) = \frac{2}{\pi^2}\frac{H_*^2}{M_P^2} \,. \tag{1.33}$$

Tensor perturbations are often normalized relative to the scalar counterpart. The tensor-to-scalar ratio is defined as

$$r \equiv \frac{\Delta_t^2(k)}{\Delta_{\mathcal{R}}^2(k)} \,. \tag{1.34}$$

Since $\Delta_{\mathcal{R}}^2$ is fixed and $\Delta_t^2 \propto H^2 \sim V$, the tensor to scalar ratio is a direct measure of the energy scale of inflation. The detection of tensor perturbations has evaded the tests of latest CMB observations, with the upper limit being constrained to the order of $r \lesssim 0.03$.

The parameters A_S, n_S and r can be directly related to the slow-roll parameters ε and

[9] We are assuming an instantaneous recombination for this qualitative analysis.

η and to the inflationary potential by substituting (1.26) into (1.32) and (1.34):

$$\begin{aligned} A_S &= \frac{1}{24\pi^2 M_P^2}\frac{V_*}{\varepsilon_*} \\ n_S - 1 &= -6\varepsilon_* + 2\eta_* \\ r &= 16\varepsilon_* \ . \end{aligned} \tag{1.35}$$

We will in fact return to those expressions in Chapters 2 and 3 in order to constrain inflationary models with CMB data.

1.1.3 Reheating

After the inflationary expansion, the Universe sits in a very low-entropy state, with its energy density consisting of a combination of the inflaton's kinetic and potential energy. As previously discussed, the initial conditions for the Hot Big Bang consist of a extremely hot, high-entropy state, populated by relativistic species. Therefore, the period of transition between the end of inflation and the onset of the radiation-dominated epoch is called reheating, where, at its end, the Universe is assigned an initial temperature T and the standard Hot Big Bang evolution follows.

The specific physical processes that took place during the reheating epoch are not entirely known. However, it is customary to visualize a standard picture, where the inflaton undergoes coherent oscillations around the minimum of its potential, ultimately dissipating energy to the Standard Model particles [Kofman et al., 1997]. As pointed out in [Kofman et al., 1994], before the perturbative decay of the inflaton, non-perturbative processes, such as parametric and non-parametric resonant decays, may have been important in the first stages of the post-inflationary expansion, called preheating.

Notwithstanding, we can perform a more general analysis of the reheating period that remains agnostic about its specific physical processes and still allows us to investigate some of its observational signatures. To this end, we can focus on the comoving Hubble radius $(a_k H_k)^{-1}$, associated with the moment a given scale $k = a_k H_k$ crossed the horizon during inflation. By following this scale's evolution from horizon crossing to the present day, we can relate it to the current Hubble radius according to [Liddle and Leach, 2003]:

$$\frac{k}{a_0 H_0} = \frac{a_k H_k}{a_0 H_0} \ . \tag{1.36}$$

We now split the right-hand side into contributions from various benchmark stages of the standard cosmic evolution. After the time inflation ends, we assume a reheating period that culminates in a radiation-dominated Universe, which lasts up to the equivalence time between radiation and matter. The instantaneous transitions between those epochs are labeled by the subscripts 'end, 'reh', 'RD' and 'eq', respectively. Thus, we re-write

equation (1.36) as

$$\begin{aligned}\frac{k}{a_0 H_0} &= \frac{a_k}{a_{end}}\frac{a_{end}}{a_{reh}}\frac{a_{reh}}{a_{RD}}\frac{a_{RD}}{a_{eq}}\frac{a_{eq}}{a_0}\frac{H_k}{H_0} \\ &= e^{-N_k} e^{-N_{reh}} e^{-N_{RD}} \frac{a_{eq}H_{eq}}{a_0 H_0}\frac{H_k}{H_{eq}} ,\end{aligned} \tag{1.37}$$

where in the last equality we explicitly wrote the number of e-folds between horizon crossing and the end of inflation, during reheating and during radiation dominance, respectively. Taking the logarithm on both sides, we have

$$\ln\left(\frac{k}{a_0 H_0}\right) = -N_k - N_{reh} - N_{RD} + \ln\left(\frac{a_{eq}H_{eq}}{a_0 H_0}\right) + \ln\left(\frac{H_k}{H_{eq}}\right) . \tag{1.38}$$

Equation (1.38) is often called the 'matching equation', as it ties together the cosmic evolution of a given scale from horizon exit during inflation to the present. We can manipulate it by following the steps developed in [Cook et al., 2015]. First, we parameterize the expansion during reheating by assuming a standard fluid description, where the evolution is dictated by an - *a priori* unknown - equation of state parameter w_{reh}. Thus, using $\rho \propto a^{-3(1+w)}$, we can express the number of e-folds during reheating as

$$N_{reh} = \frac{1}{3(1+w_{reh})} \ln\left(\frac{\rho_{end}}{\rho_{reh}}\right) , \tag{1.39}$$

where ρ_{end} and ρ_{reh} are the energy densities at the end of inflation and at the end of reheating, respectively. We can write $\rho_{end} = \frac{3}{2}V_{end}$ by making $w_\phi = -1/3$ at the end of inflation[10]. Also, from fluid thermodynamics we can change from the energy density to the temperature at the end of reheating according to $\rho_{reh} = \frac{\pi^2}{30} g_{reh} T_{reh}^4$, with g_{reh} being the effective number of relativistic species at the onset of the radiation dominated epoch. Therefore, we write N_{reh} as

$$N_{reh} = \frac{1}{3(1+w_{reh})} \ln\left(\frac{45}{\pi^2}\frac{V_{end}}{g_{reh}T_{reh}^4}\right) . \tag{1.40}$$

As the temperature at the end of reheating T_{reh}, i.e at the beginning of the Hot Big Bang, is subject to large uncertainties, we can explore the conservation of entropy in the radiation gas to replace it for the cosmic temperature today. Therefore, taking into account the change in helicity states from reheating to today, we make

$$T_{reh} = T_0 \left(\frac{a_0}{a_{reh}}\right)\left(\frac{43}{11 g_{reh}}\right)^{1/3} = T_0 \left(\frac{a_0}{a_{eq}}\right) e^{N_{RD}} \left(\frac{43}{11 g_{reh}}\right)^{1/3} . \tag{1.41}$$

[10] Notice that $w < -1/3$ is the requirement that the eos parameter of the inflaton must satisfy in order to accelerate the Universe. Thus, when $w = -1/3$ inflation ends.

Now, plugging (1.41) into (1.40), we get:

$$\frac{3(1+w_{reh})}{4}N_{reh} = \ln(V_{end})^{1/4} - \frac{1}{4}\ln\left(\frac{\pi^2}{45}g_{reh}\right) - \ln\left(\frac{T_0 a_0}{a_{eq}}\right) - \frac{1}{3}\ln\left(\frac{43}{11 g_{reh}}\right) - N_{RD} \ . \tag{1.42}$$

We would like to obtain an expression that relates N_k to N_{reh} only. To this end, we can eliminate the dependence on N_{RD} by isolating it from the matching equation (1.38) and substituting in (1.42). After some algebraic manipulations, we finally get

$$N_k = \frac{-1+3w_{reh}}{4}N_{reh} - \ln\left(\frac{V_{end}^{1/4}}{H_k}\right) - \frac{1}{4}\ln\left(\frac{45}{\pi^2 g_{reh}}\right) + \frac{1}{3}\ln\left(\frac{43}{11 g_{reh}}\right) - \ln\left(\frac{k}{a_0 T_0}\right) \ . \tag{1.43}$$

The last three terms in the above expression are, in principle, fixed by assuming standard ΛCDM Cosmology. Hence, inserting $g_{reh} \approx 100$, $T_0 = 2.7$ K and choosing the pivot scale of $k = 0.05$ Mpc^{-1}, we obtain

$$N_k = \frac{-1+3w_{reh}}{4}N_{reh} - \ln\left(\frac{V_{end}^{1/4}}{H_k}\right) + 61.55 \ . \tag{1.44}$$

The first two terms in the right-hand side are model-dependent, as one would need to specify an equation of state parameter for the reheating stage as well as a specific inflationary potential. An useful guide is to consider a power-law potential $V(\phi) \propto |\phi|^n$ for the oscillatory phase during reheating. Under this approximation, it was shown in [Turner, 1983] that for large time scales, the field oscillations average out to mimic an expansion period dominated by a fluid with equation of state parameter

$$w_{reh} = \frac{n-2}{n+2} \ . \tag{1.45}$$

In Chapter 3, we will show that for our inflationary potential under consideration, the evolution after inflation is dictated by an approximately quadratic, followed by an approximately quartic potential. Ultimately, that allows us to use (1.45) to assign an effective matter-dominated and radiation-dominated splits to the reheating stage, which will be useful to quantitatively constrain the inflationary e-fold number from a general reheating analysis.

1.2 The ΛCDM Model

The current concordance model of Cosmology is the result of several surprising discoveries in the last century. In 1933, astronomer Fritz Zwicky pointed that the sum of the masses of all the stars in the Coma cluster was not enough to prevent the galaxies from escaping the cluster's gravitational pull [Zwicky, 1933]. This became known as the

missing mass problem, and was an astronomical puzzle for many years. In the 1970s, a group led by astronomer Vera Rubin helped to shed more light into the issue [Rubin et al., 1978]. They observed that the mass of all the stars within a typical galaxy could not account for the mass needed to keep the stars orbiting the galactic center. Therefore, there must be some kind of exotic, non-luminous matter constituent in the Universe, which was dubbed as dark matter. It does not radiate, so we can only infer its existence from its gravitational influence. It was not clear, however, what was the extent of the role dark matter would play in the grand scheme of the cosmos.

Since the end of the 1990s and early 2000s, Cosmology started to greatly benefit from high-precision measurements, from both early- and late-time surveys. Ultimately, that allowed us to unveil the dynamics of large-scale structure - and consequently its energy content - with great accuracy. Observations of gravitational lensing - the bending of background light passing near a massive object - showed that dark matter composes the majority of the gravitational matter we observe in the Universe. Also, from CMB measurements, it became clear that dark matter had to be present in the early Universe, so that it could provide the gravitational potential wells necessary for the formation of large-scale structure. From the particle physics standpoint, there are ongoing efforts to find a dark matter particle in the current particle accelerators, while many alternatives have been proposed for dark matter in Beyond the Standard Model Physics.

Another breakthrough happened in 1998, when a group led by Adam Riess discovered that light coming from distant Type Ia Supernovae (SNIa) appeared dimmer than expected, based on standard cosmological assumptions [Riess et al., 1998]. Since SNIa are standardized candles, i.e objects with well-determined luminosity, we can directly infer their distance from the measured flux[11], so the SNIa were also farther away than anticipated. Considering the range of distances probed by the experiment, this effect must come from a cosmological origin, pointing to a discrepancy between the assumed cosmological expansion and the novel data. A solution appears if one assumes that the Universe is currently undergoing an accelerated expansion. It has the effect of increasing the physical distance that light has to travel from a SNIa event to us, explaining the weakening of its light intensity. Since we know that a cosmic fluid composed of any of the SM particles does not produce this effect, this acceleration must be propelled by an exotic component of the Universe, called dark energy. In the context of classic GR, the simplest way to give origin to a dark energy component is by introducing a constant Λ into the Einstein-Hilbert lagrangian, which gives rise to an extra term in the action (1.1):

$$S = \frac{M_P^2}{2} \int d^4x \sqrt{-g}(R - 2\Lambda) \ . \tag{1.46}$$

[11] The integrated flux coming from all wavelenghts is $f = \frac{L}{4\pi d^2}$, where L is the objects' intrinsic luminosity and d its distance.

The Friedman equation (1.5) is modified accordingly:

$$H^2(t) = \frac{1}{3M_P^2}(\rho(t) + \rho_\Lambda) - \frac{k}{a^2} \,, \tag{1.47}$$

where $\rho_\Lambda \equiv M_P^2\Lambda$ is the (constant) density of dark energy. Note that, according to the conservation equation (1.7) with $\dot{\rho}_\Lambda = 0$ we find $p_\Lambda = -\rho_\Lambda$. Hence, the cosmological constant behaves as a fluid with negative pressure, contributing to a positive acceleration for the Universe. From the theoretical point of view, one could interpret Λ as vacuum energy density, resulting from the zero-point energy of all quantum fields in nature. However, the inferred value from cosmological measurements is ~ 120 order of magnitudes smaller than expected from quantum field theoretical calculations. This enormous discrepancy is called the cosmological constant problem and still motivates several discussions regarding the true nature of dark energy.

In terms of the density parameter $\Omega_\Lambda = \rho_\Lambda/\rho_c$, we can rewrite equation (1.10) as

$$H^2(a) = H_0^2(\Omega_m a^{-3} + \Omega_\Lambda) \,, \tag{1.48}$$

where $\Omega_m = \Omega_b + \Omega_c$ is the matter density parameter in terms of the baryonic and dark matter fractional density. We have also dropped the radiation term, which is negligible nowadays $\Omega_r \sim 10^{-4}$ and spatial curvature, which is diluted to zero due to inflation.

In order to be constrained with large-scale observations, the ΛCDM model assumes six free parameters: the amplitude of primordial scalar perturbations A_S; the scalar spectral index n_S; the physical baryon density and matter densities: $\omega_b \equiv \Omega_b h^2$ and $\omega_m \equiv \Omega_m h^2$[12]; the cosmological constant density parameter Ω_Λ and the integrated optical depth to recombination τ, which affects the propagation of CMB photons through the ionizing effect of the first generation of stars. Their measured values are in Table 1.1.

Parameter	Value
$10^9 A_S$	2.198 ± 0.085
n_S	0.967 ± 0.004
$100\omega_b$	2.242 ± 0.014
$100\omega_m$	14.24 ± 0.009
Ω_Λ	0.689 ± 0.006
τ	0.056 ± 0.007

Table 1.1: Parameters of ΛCDM Cosmology [Baumann, 2022].

Thus, the current concordance picture of Cosmology is that we are currently living in a spatially flat Universe, dominated by a cosmological constant, with most of the matter density in form of dark matter and a small fraction of ordinary baryonic matter.

[12]The parameter h is the dimensionless Hubble constant, defined as $H_0 \equiv 100h$ km s^{-1} Mpc^{-1}

1.2.1 Current Cosmological Tensions

As mentioned, the ΛCDM model faces the challenge of providing a satisfactory physical interpretation for the nature of dark matter and dark energy. Apart from these theoretical issues, the model has also been questioned from the observational front in the last decade, with non-trivial discrepancies between early- and late-time surveys.

The currently most significant cosmological tension is focused on the present-day expansion rate, the Hubble constant H_0. It is most directly measured by observations of nearby objects, up to redshifts $z \sim 0.1$, or distances of ~ 100 Mpc. Since it is a probe of the local Universe, it does not require knowledge of the whole dynamics of the expansion rate $H(z)$, so we can Taylor expand the scale factor $a(t)$ around its present value:

$$\begin{aligned} a(t) &= a(t_0) + \dot{a}(t_0)(t - t_0) + \dots \\ \implies \frac{a(t)}{a(t_0)} &- 1 = H_0(t - t_0) + \dots \ . \end{aligned} \tag{1.49}$$

Using the definition of the cosmological redshift $z \equiv \frac{a(t)}{a(t_0)} - 1$, we can write the above expression up to first order as

$$z = H_0 d_L + \dots \ , \tag{1.50}$$

where, $d_L = t - t_0$ is, in natural units, the distance traveled by a light signal sent from some time t in the past. This equation was employed by Edwin Hubble, in the 1930s, in the process of finding evidence for an expanding Universe, using the redshift of light coming from receding nearby galaxies. Nowadays, a similar version, with higher order terms, is used in order to assess slightly more distant objects:

$$d_L = H_0^{-1}\left[z + \frac{1}{2}(1 - q_0)z^2 - \frac{1}{6}(1 - q_0 - 3q_0^2 + j_0)z^3\right] \ . \tag{1.51}$$

The parameters q_0 and j_0 are related to higher order derivatives of the scale factor.

In this century, the SH0ES collaboration [Riess et al., 2022], using the Hubble Space Telescope, was able to build a distance ladder and establish a distance-redshift relation (1.51) with observations of SNIa, callibrated with Cefeids in the Large Magellanic Cloud. Their best-fit value for the Hubble constant is $H_0 = 73.04 \pm 1.04$ km s^{-1} Mpc^{-1}.

Another possibility of measuring the Hubble constant is by assessing the distant Universe, through observations of the Cosmic Microwave Background. In section 1.1.2 we discussed how the CMB temperature power spectrum is able to constrain the parameters of a cosmological model. However, our discussion of ΛCDM did not include the Hubble constant as a free parameter. Since the Friedmann equation (1.48) relates H_0 to the density parameters Ω_m and Ω_Λ, we can make Ω_Λ a derived parameter and substitute

$\Omega_\Lambda = 1 - \Omega_m$[13] back into (1.48):

$$\frac{H^2(a)}{(100 \text{ km s}^{-1} \text{ Mpc}^{-1})^2} = \omega_m(a^{-3} + 1) + h^2 \,. \tag{1.52}$$

The parameter-dependence in the above expression for the expansion rate changes the distance to the last-scattering surface, which affects the peak locations in the CMB spectrum. The physical matter density ω_m is well constrained by the height of the first few peaks in the power spectrum. Therefore, in order to maintain the peak locations, the CMB spectrum requires a Hubble constant of $H_0 = 67.36 \pm 0.54$ km s^{-1} Mpc^{-1} [Aghanim et al., 2020a].

This last result represents a discrepancy of $\sim 4\sigma$ with the value from the discussed local distance-ladder measurements, known as the Hubble constant tension. One might wonder if this disagreement is a consequence of systematic errors in the datasets, but this conjecture cannot solve the tension alone [Di Valentino et al., 2021c]. On the other hand, this picture might be an evidence of beyond ΛCDM signatures in Cosmology. Several scenarios have been proposed in order to resolve or alleviate the tension [Di Valentino et al., 2021a]. However, modifying the standard cosmological model in an effort to account for the H_0 tension has proven to be rather difficult, given the success of the six-parameter ΛCDM in satisfying the constraints from a multitude of datasets.

Another cosmological parameter that has been at the center of recent observational discrepancies is the clustering parameter σ_8. It measures the amplitude of matter perturbations at the scale of 8 h^{-1} Mpc, and is given by [Dodelson, 2003]:

$$\sigma_8 \equiv [\langle \delta^2_{m,8} \rangle]^{1/2} = \left[\frac{1}{2\pi^2} \int d\ln k k^3 P(k) |W(k)|^2 \right]^{1/2} \,, \tag{1.53}$$

with δ_m being the density contrast of matter perturbations and $W(k)$ the window function. The linear matter power spectrum, $P(k)$ encodes the evolution of scales throughout cosmic history, making the clustering parameter dependent on the cosmological model.

Lower redshift assessments of σ_8 involves weak gravitational lensing measurements, which affects the shapes of observed galaxies. On cosmological scales, we can use this effect to better understand the matter distribution of the Universe. Since this is a more direct probe of matter perturbations, one can use the definition in (1.53) to constrain the clustering parameter. It is often quantified in terms of $S_8 \equiv \sigma_8 \sqrt{\Omega_m / 0.3}$, where Ω_m is the overall matter density parameter. In particular, the Kilo-Degree Survey (KiDS-1000) lensing estimation reported a clustering value of $S_8 = 0.759^{+0.024}_{-0.021}$ [Asgari et al., 2021].

On the other hand, we can also investigate the clustering of matter through observations of the CMB. Since the CMB power spectrum places tight constraints on the cosmo-

[13] This comes from evaluating the Friedmann equation (1.48) in the present day, which yealds $1 = \Omega_m + \Omega_\Lambda$.

logical parameters, it also probes the amplitude and growth of the matter distribution, hence, σ_8. This model-dependent estimation, however, is sensitive to other parameters that might affect the clustering of matter, such as the optical depth to reionization τ [Di Valentino et al., 2021b]. Assuming flat ΛCDM, CMB data seem to prefer a larger amount of matter clustering, returning a value of $S_8 = 0.834 \pm 0.016$ [Aghanim et al., 2020a], which shows a discrepancy of $\sim 3\sigma$ with weak lensing measurements.

The usual theoretical approach to aleviate the S_8 tension involves modifying the matter sector of ΛCDM. However, any modification of Ω_m also induces a modification of the CMB-inferred value of H_0, given the tight constraints on the physical matter density $\omega_m = \Omega_m h^2$, known as geometric degeneracy. In turn, this produces a modification of distances to sources, of the sound horizon, the growth of matter and CMB anisotropies, which usually result in a higher value of σ_8 due to an extended period of matter domination [Di Valentino et al., 2021b]. Hence, the H_0 and S_8 tensions are correlated, and proposals applied to alleviate one usually tend to exacerbate the other. It goes without saying that finding a solution to the discrepancies on both of these parameters is troublesome. We will return to this discussion in Chapter 3.

Chapter 2

Aspects of Higgs Inflation

So far, among the fundamental forces of nature, everything discussed was only concerned with the gravitational interaction and its effect on large-scale structure. As gravity is currently portrayed by the laws of General Relativity, the strong force, the weak force and electromagnetism, are described by what is called the Standard Model of Particle Physics (SM). The structure of the SM is the result of many developments in Quantum Field Theory and Group Theory in the last century [Pais, 1986]. The former incorporates the rules of quantum mechanics and special relativity to fundamental fields and, in a phenomenological point of view, allows one to compute amplitudes for numerous elementary particle processes; while the latter allows us to write the SM lagrangian by means of symmetry arguments. In this sense, this lagrangian is made invariant with respect to the set of transformations:

$$\text{Poincaré} \times SU_C(3) \times SU_L(2) \times U_Y(1) \ . \tag{2.1}$$

The first term in (2.1) refers to the Poincaré group, which, ultimately, is responsible for assigning the spin of elementary particles[1] and establishing the structure of the free lagrangian. The remaining groups in (2.1) are *gauge* groups, which have the role of adding interaction terms to the lagrangian, expressed in terms of *gauge* fields. $SU_C(3)$ is the symmetry group of the theory of quantum chromodynamics (QCD), which governs the interaction of charged color particles (quarks) with gluons. $SU_L(2) \times U_Y(1)$ is the electroweak sector, acting on left-handed chirality particles that carry the hypercharge quantum number. All matter particles are charged under the $SU_L(2) \times U_Y(1)$ symmetry.

The matter particles of the SM are collectively called fermions. They are described by spin-1/2 fields and are divided into quarks and leptons. Quarks carry color charge and therefore are charged under both QCD and electroweak interactions. Leptons do not carry color charge and are just part of the electroweak sector. The force mediator particles are

[1] Particles of different spin are associated with different representations of the ortochronous Lorentz group, contained in the larger Poincare group.

represented by spin-1 fields and are called gauge bosons. They are the gluon of QCD, the W^+, W^- and Z of weak interaction phenomena, and the photon of electromagnetism.

This whole puzzle of the SM particles, interactions and symmetries was completed in the 1970s, after the establishment of the Higgs mechanism and electroweak symmetry breaking. This is where the Higgs boson, the main character of our discussion, came into play.

2.1 The Higgs in the Standard Model of Particle Physics

In the 1950s, a group led by Chien-Shiung Wu [Wu et al., 1957] discovered a violation of the parity symmetry in processes involving the weak interaction. Later, Richard Feynman and Murray Gell-Mann [Feynman and Gell-Mann, 1958] proposed a theory in which only left-handed particles (and right-handed antiparticles) are charged under the weak force, which would account for the observed violation of parity. A profound consequence is that all fermions of the SM should be fundamentally massless[2]. Evidently, that is not the case. A solution was put forward by Higgs-Brout-Angels [Englert and Brout, 1964, Higgs, 1964] and, independently, by Guralnik-Hagen-Kibble [Guralnik et al., 1964] in 1964, in which a new field, the Higgs, was introduced. In the fundamental theory, at high energies, every field is massless. Particles that couple to the Higgs would gain their masses in a spontaneous symmetry breaking (SSB) process of the Higgs potential. This mechanism is also incorporated in the unification of the electromagnetic and weak interactions, the electroweak model of Weinberg-Glashow-Salam [Glashow, 1959, Salam, 1968, Weinberg, 1967]. Thus, the electroweak sector of the SM symmetry groups in (2.1) is spontaneously broken into the known electromagnetic $U(1)$ gauge group, according to:

$$SU_L(2) \times U_Y(1) \xrightarrow{\text{SSB}} U_{\text{EM}}(1) \, . \tag{2.2}$$

The spontaneous symmetry breaking process is formulated in terms of the dynamics of the Higgs field. A potential that can give rise to such mechanism is

$$V(\phi) = \frac{\mu^2}{2}\phi^2 + \frac{\lambda}{4}\phi^4 \, , \tag{2.3}$$

in which $\phi^2 = \Phi^\dagger\Phi$. $\Phi = \begin{pmatrix} \phi^{(+)} \\ \phi^{(0)} \end{pmatrix}$ is the Higgs $SU(2)$ doublet and the superscripts reflect the electric charges of each Higgs component.[3] This potential can, in fact, undergo SSB

[2] A spinor mass term represented by $\mathcal{L} \supset m\bar{\psi}\psi = m\bar{\psi}_L\psi_R + m\bar{\psi}_R\psi_L$ is not allowed in chiral theories (such as the one proposed by [Feynman and Gell-Mann, 1958]), since it explicitly mixes right- and left-handed spinors.

[3] This is based on the Higgs coupling with the other SM fields, so that all interaction terms conserve

if $\mu^2 < 0$, as shown in Figure 2.1.

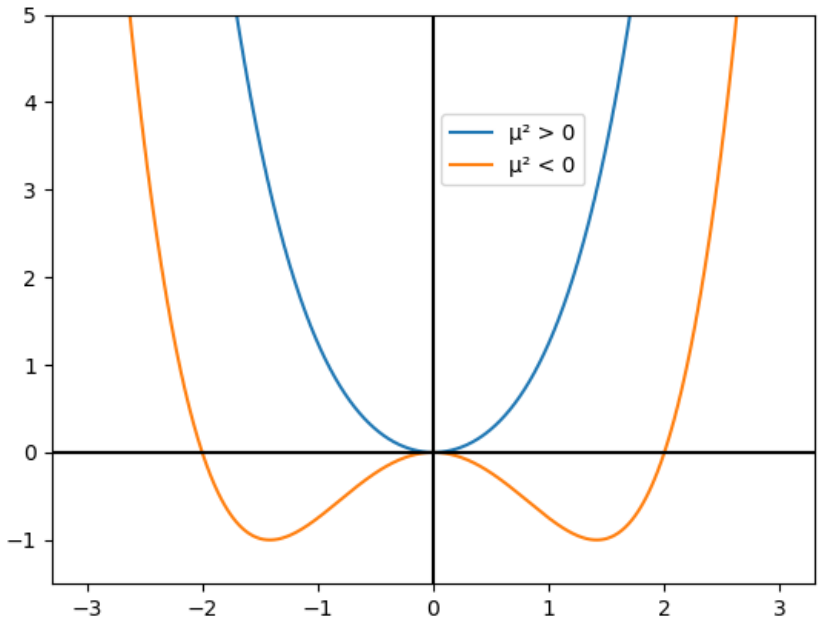

Figure 2.1: Higgs potential (2.3).

Notice that a transition between the regimes of $\mu^2 > 0$ and $\mu^2 < 0$ is associated with an evolution of the minimum of the potential - obtained by solving $\frac{\partial V}{\partial \phi} = 0$ - at $\phi = 0$, to the minima at $\phi = \pm\sqrt{-\frac{\mu^2}{\lambda}}$. Under this last vacuum configuration, the symmetries of (2.1) are not realized anymore. Instead, they are reduced to (2.2), and we say that a spontaneous symmetry breaking has occurred.

This non-trivial vacuum configuration is only possible because the Higgs is a scalar field, associated with a spin-0 particle. One cannot attribute a non-zero VEV for fermions or vector bosons because they possess non-trivial spin, which would imply in a breaking of Lorentz symmetry (vacuum should be orthogonal to non-zero spin states). For the same reason, we infer that the Higgs VEV ought to be represented by the neutral component of the Higgs doublet, since the vacuum should be electric neutral. Therefore, we can propose a general parametrization of the Higgs doublet in vacuum as

$$\Phi = \begin{pmatrix} 0 \\ \frac{v}{\sqrt{2}} \end{pmatrix} , \tag{2.4}$$

where $v \approx 246$ GeV is the Higgs VEV. As mentioned earlier, the symmetry breaking process is associated with the generation of fermion and vector boson masses. That can be seen through their coupling with the Higgs after SSB.

electric charge.

First, let us consider a generic lepton[4] generation coupled to the Higgs doublet (2.4). The lepton $SU_L(2)$ doublet is $L = \begin{pmatrix} \nu_L^l \\ l_L \end{pmatrix}$, where l_L and ν_L^l are the lepton's and the lepton neutrino's left-handed components, respectively. The right-handed counterpart is a $SU_L(2)$ singlet l_R[5]. The interaction term with the Higgs can be written as [Schwartz, 2014]

$$\begin{aligned} \mathcal{L} \supset y_l \bar{L} \Phi l_R + \text{h.c.} &= y_l \begin{pmatrix} \bar{\nu}_L^l & \bar{l}_L \end{pmatrix} \begin{pmatrix} 0 \\ \frac{v}{\sqrt{2}} \end{pmatrix} l_R + \text{h.c.} \\ &= m_l(\bar{l}_L l_R + \bar{l}_R l_L), \qquad m_l = y_l \frac{v}{\sqrt{2}} \, , \end{aligned} \tag{2.5}$$

where m_l is the lepton's mass and y_l the lepton's Yukawa coupling. Thus, a coupling with the Higgs produces, after SSB, a lepton mass proportional to the Higgs VEV.

In the case of gauge bosons, we first start by writing the lagrangian for the gauge fields' kinetic terms and the Higgs sector:

$$\mathcal{L} \supset -\frac{1}{4}(W_{\mu\nu}^a)^2 - \frac{1}{4}B_{\mu\nu}^2 + (D_\mu \Phi)^\dagger (D^\mu \Phi) + V(\Phi) \, , \tag{2.6}$$

with $W_{\mu\nu}^a = \partial_\mu W_\nu^a - \partial_\nu W_\mu^a - g\epsilon^{abc} W_\mu^b W_\nu^c$ and $B_{\mu\nu} = \partial_\mu B_\nu - \partial_\nu B_\nu$ being the $SU(2)$ and $U(1)$ field strenghts, respectively. $W_\mu^a = W_\mu^1, W_\mu^2, W_\mu^3$ and B_μ are, respectively, the $SU(2)$ and $U(1)$ gauge fields.

The generation of masses can be visualized by the definition of the Higgs covariant derivative, $D_\mu \Phi$, appearing in the above lagrangian. The procedure of introducing interactions in the SM involves localizing a gauge symmetry[6], such as the ones of (2.1). After this, in the interesting of keeping the lagrangian gauge invariant, one is forced to redefine the derivatives in terms of a more general covariant derivative. Since the Higgs is charged under both $SU_L(2)$ and $U_Y(1)$, its covariant derivative features the gauge fields of both these symmetry groups:

$$D_\mu \Phi = \partial_\mu \Phi - \frac{i}{2} g W_\mu^a \sigma^a \Phi - \frac{i}{2} g' B_\mu \Phi \, . \tag{2.7}$$

Here, g and g' are the $SU(2)$ and $U(1)$ couplings, respectively. $\sigma^a = \sigma^1, \sigma^2, \sigma^3$ are the $SU(2)$ generators, often called the Pauli matrices in the fundamental representation. Therefore, the kinetic term for the Higgs $(D_\mu \Phi)^\dagger (D^\mu \Phi) = |D_\mu \Phi|^2$, using (2.4) and

[4] The generation of quark masses is still understood in terms of the Higgs mechanism but is a little more involved due to the mass (CKM) mixing matrix [Schwartz, 2014]. For our purposes, we can focus on leptons.

[5] Right-handed neutrinos have never been observed so they are not included in the SM.

[6] The gauge symmetry groups in (2.1) define a set of transformations that preserve said symmetry. These transformations can be effectively described by a set of generators and parameters. Localizing the symmetry means making these parameters space-time dependent.

(2.7) reads [Schwartz, 2014]

$$\begin{aligned}\mathcal{L} \supset |D_\mu \Phi|^2 =& g^2 \frac{v^2}{8} \begin{pmatrix} 0 & 1 \end{pmatrix} \begin{pmatrix} \frac{g'}{g} B_\mu + W_\mu^3 & W_\mu^1 - i W_\mu^2 \\ W_\mu^1 + i W_\mu^2 & \frac{g'}{g} B_\mu - W_\mu^3 \end{pmatrix} \\ & \times \begin{pmatrix} \frac{g'}{g} B_\mu + W_\mu^3 & W_\mu^1 - i W_\mu^2 \\ W_\mu^1 + i W_\mu^2 & \frac{g'}{g} B_\mu - W_\mu^3 \end{pmatrix} \begin{pmatrix} 0 \\ 1 \end{pmatrix} \\ =& g^2 \frac{v^2}{8} \left[(W_\mu^1)^2 + (W_\mu^2)^2 + \left(\frac{g'}{g} B_\mu - W_\mu^3 \right)^2 \right] .\end{aligned} \tag{2.8}$$

These terms are quadratic in the gauge fields, so we can identify them as mass terms. However, the masses must be diagonalized. This can be done under the set of field redefinitions:

$$\begin{aligned} Z_\mu &\equiv \cos\theta_W W_\mu^3 - \sin\theta_W B_\mu 3 \\ A_\mu &\equiv \sin\theta_W W_\mu^3 + \cos\theta_W B_\mu^3 \\ W_\mu^\pm &\equiv \frac{1}{\sqrt{2}} (W_\mu^1 \mp i W_\mu^2) , \end{aligned} \tag{2.9}$$

where θ_W is the Weinberg angle. With the fields (2.9) and the covariant derivative (2.8), we can rewrite the lagrangian (2.6) as

$$\begin{aligned} \mathcal{L} \supset -\frac{1}{4} F_{\mu\nu}^2 - \frac{1}{4} Z_{\mu\nu}^2 + \frac{1}{2} m_Z^2 Z^\mu Z_\nu - \frac{1}{2} (\partial_\mu W_\nu^+ - \partial_\nu W_\mu^+)(\partial_\mu W_\nu^- - \partial_\nu W_\mu^-) + m_W^2 W_\mu^+ W^{\mu -}, \\ m_Z = \frac{g}{2\cos\theta_W} v, \qquad m_W = \frac{g}{2} v . \end{aligned} \tag{2.10}$$

Therefore, the above lagrangian tells us that, after SSB, the gauge bosons Z and $W^\pm$ also acquire masses proportional to the Higgs VEV. The one combination in (2.9) that does not gain mass is precisely the electromagnetic photon A_μ.

Thus, the Higgs mechanism provides a way of breaking the electroweak symmetry, generating both the phenomenology of the weak interactions mediated by massive vector bosons, and ordinary electromagnetism with the massless photon. Also, thorugh the Yukawa couplings, the Higgs VEV also generates mass to the fermions of the SM. This whole machinery has been well tested and supported experimentaly, especially with the discovery of the Higgs at the LHC in 2012 [Aad et al., 2012].

2.2 The Higgs as the Inflaton

Keeping in mind the discussion of Chapter 1, the idea of promoting the Higgs boson to the status of the inflaton is tempting, since it is the only scalar particle in the SM.

Thus, it is not surprising that this hypothesis has been raised by several authors in the recent past [Barbon and Espinosa, 2009, Bezrukov and Shaposhnikov, 2008, Burgess et al., 2010]. Unfortunately, the potential (2.3) is poorly constrained by CMB measurements, as it requires a value for the Higgs quartic coupling far too small $\lambda \sim 10^{-13}$ to reproduce the observed amplitude of the primordial power spectrum. Therefore, in 2008, Bezrukov and Shaposhnikov proposed a new Higgs inflationary potential, which had the novel feature of a non-minimal coupling between the Higgs and gravity [Bezrukov and Shaposhnikov, 2008]. The action is then given by (1.17), where we now denote the Higgs scalar as h, more commonly used in the literature:

$$\begin{aligned} S &= \int d^4x\sqrt{-g}\left[R - \frac{1}{2}\partial_\mu h\partial^\mu h - V(h)\right], \\ V(h) &= \frac{\mu^2}{2}h^2 + \frac{\lambda}{4}h^4 + \frac{1}{2}\xi h^2 R\,, \end{aligned} \tag{2.11}$$

where ξ is the non-minimal coupling parameter. The addition of the non-minimal term considerably increases the difficulty in manipulating the dynamic equations related to such potential. Therefore, it is customary in the literature to perform a change of variables, both in the metric and in the scalar field, in order to simplify the analysis. With regard to the metric $g_{\mu\nu}$, we employ a conformal transformation of the type [Faraoni et al., 1999]:

$$g_{\mu\nu} \to \tilde{g}_{\mu\nu} = \Omega^2(x) g_{\mu\nu}\,, \tag{2.12}$$

with $\Omega(x)$ being a spacetime-dependent conformal factor. The transformation (2.12) corresponds to a local rescaling of spatial and temporal distances. The action (2.11), which is a function of the original metric $g_{\mu\nu}$, is referred to as the Jordan frame action, whereas the action as a function of the conformally transformed metric $\tilde{g}_{\mu\nu}$ is called the Einstein frame action. Naturally, the metric determinant g and the Ricci scalar R are going to change under the conformal transformation. Following the steps developed in [Garcia-Bellido et al., 2009], under the transformation (2.12), the action (2.11) transforms as

$$S_J \to S_E = \int d^4x\sqrt{-g}\left\{\frac{M_P^2 + \xi h^2}{2\Omega^2}\left[\tilde{R} + 3\tilde{\Box}\ln\Omega^2 - \frac{3}{2}\tilde{g}^{\mu\nu}\tilde{\nabla}_\mu \ln\Omega^2 \tilde{\nabla}_\nu \ln\Omega^2\right] - \frac{\tilde{\partial}_\mu h \tilde{\partial}^\mu h}{2\Omega^2} - \frac{V_J(h)}{\Omega^4}\right\}. \tag{2.13}$$

We can conveniently choose the conformal factor in order to recover the usual Einstein-Hilbert term. Thus, we make:

$$\Omega^2(h) = 1 + \frac{\xi h^2}{M_P^2}\,. \tag{2.14}$$

Under this specific transformation, the action above reduces to

$$S_E = \int d^4x\sqrt{-\tilde{g}}\left\{\frac{M_P^2}{2}\tilde{R} - \frac{1}{2}\left[\frac{\Omega^2 + 6\xi^2 h^2/M_P^2}{\Omega^4}\right]\tilde{g}^{\mu\nu}\partial_\mu h\partial_\nu h - \frac{V_J(h)}{\Omega^4}\right\}\,, \tag{2.15}$$

where we have omitted the specific form of Ω^2 to keep the expression cleaner. The last step is getting rid of the non-minimal kinetic term for the scalar field. To this end, we can perform a field redefinition:

$$h \to \chi, \quad \frac{d\chi}{dh} = \sqrt{\frac{\Omega^2 + 6\xi^2 h^2/M_P^2}{\Omega^4}} = \sqrt{\frac{1 + \xi(1+6\xi)h^2/M_P^2}{(1+\xi h^2/M_P^2)^2}}\,. \tag{2.16}$$

As we will most generally investigate the scalar field dynamics during inflation in the Einstein frame, we drop the tilde notation from now on. The action in the Einstein frame, as a function of the new scalar field χ, reads:

$$\begin{aligned} S_E &= \int d^4x\sqrt{-g}\left[\frac{M_P^2}{2} - \frac{1}{2}\partial_\mu\chi\partial^\mu\chi - V_E(\chi)\right], \\ V_E(\chi) &= \frac{1}{\Omega^4(h(\chi))}V_J(h(\chi))\,. \end{aligned} \tag{2.17}$$

Note that the action has recovered the usual minimal coupling of the scalar field with gravity. The Einstein frame potential is obtained from the Jordan frame potential (2.11) and the conformal factor $\Omega^2(h) = 1 + \frac{\xi h^2}{M_P^2}$, where the dependence in h must be changed to a dependence in χ according to (2.16). This can be done by direct integration, which yields

$$\frac{\sqrt{\xi}}{M_P}\chi(h) = \sqrt{1+6\xi}\sinh^{-1}(\sqrt{1+6\xi}u) - \sqrt{6\xi}\sinh^{-1}\left(\sqrt{6\xi}\frac{u}{\sqrt{1+u^2}}\right)\,, \tag{2.18}$$

where $u \equiv \sqrt{\xi}M_P$. We can work in the large coupling regime (which will be justified later) and assume $\xi \gg 1$. Thus, $1 + 6\xi \approx 6\xi$, and we can use the identity $\sinh^{-1}x = \ln(x + \sqrt{x^2+1})$ to approximate equation (2.18) to

$$\begin{aligned} \chi(h) = \sqrt{6}M_P\ln\sqrt{1+\xi h^2/M_P^2} &= \sqrt{6}M_P\ln\Omega, \\ \implies \Omega^2(\chi) &= e^{\sqrt{\frac{2}{3}}\frac{\chi}{M_P}}\,. \end{aligned} \tag{2.19}$$

Therefore, the approximation $\xi \gg 1$ allows us to express the conformal factor in terms of the new field χ in a very simple way. Hence, we can use (2.17) to write the Einstein frame potential as

$$V_E(\chi) = \frac{\lambda M_P^4}{4\xi^2}\left[e^{\sqrt{\frac{2}{3}}\frac{\chi}{M_P}} - \left(1 + \xi\frac{v^2}{M_P^2}\right)\right]^2 e^{-2\sqrt{\frac{2}{3}}\frac{\chi}{M_P}}\,. \tag{2.20}$$

Since $v \ll M_P$ we can approximate $1 + \xi\frac{v^2}{M_P^2} \approx 1$ and effectively write the inflationary potential as

$$V(\chi) = \frac{\lambda M_P^2}{4\xi^2}\left(1 - e^{-\sqrt{\frac{2}{3}}\frac{\chi}{M_P}}\right)^2 . \tag{2.21}$$

The potential (2.21) is valid for the region $\chi > 0$, which is relevant for inflation[7]. This form of the Higgs inflationary potential was first studied in [Bezrukov and Shaposhnikov, 2008] and is plotted in Figure 2.2. Notice that the flat region consistent with slow-roll inflation is achieved for large field values.

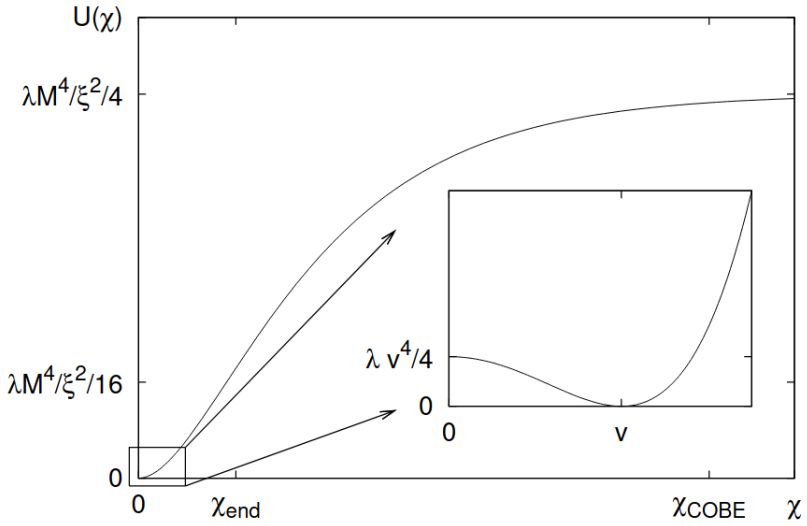

Figure 2.2: The Higgs inflationary potential (2.21) [Bezrukov and Shaposhnikov, 2008].

To quantitatively check weather this model can successfully achieve slow-roll inflation, we develop the usual analysis in terms of the slow-roll parameters. Therefore, substituting the potential and its derivatives into (1.26), we get

$$\begin{aligned} \epsilon &= \frac{4}{3}(e^{\sqrt{\frac{2}{3}}\frac{\chi}{M_P}} - 1)^{-2} = \frac{4M_P^4}{3\xi^2 h^4} \\ \eta &= \frac{4}{3}\frac{(2 - e^{\sqrt{\frac{2}{3}}\frac{\chi}{M_P}})^2}{e^{\sqrt{\frac{2}{3}}\frac{\chi}{M_P}} - 1} = -\frac{4M_P^2}{3\xi h^2} . \end{aligned} \tag{2.22}$$

The slow-roll conditions $\{\epsilon, \eta\} \ll 1$ translate to the field regime during inflation, which is $\chi \gg \sqrt{6}M_P$, or, equivalently, $h \gg M_P/\sqrt{\xi}$. As always, we can find the field value at the end of inflation by making $\epsilon \simeq 1$, corresponding to $h_{end} \simeq (4/3)^{1/4} M_P/\sqrt{\xi} \simeq 1.07 M_P/\sqrt{\xi}$. The inflationary e-fold number, which quantifies the expansion from horizon crossing of

[7] As discussed in [Garcia-Bellido et al., 2009], the conformal transformation is ill-defined for negative field values.

a given scale to the end of inflation, is given in terms of the potential according to (1.28):

$$N_k = \int_{h_{end}}^{h_0} \frac{1}{M_P^2} \frac{V}{dV/dh} \left(\frac{d\chi}{dh}\right)^2 dh \simeq \frac{3}{4} \frac{h_0^2 - h_{end}^2}{M_P^2/\xi} \ . \tag{2.23}$$

The authors in [Bezrukov and Shaposhnikov, 2008] fixed the number of e-folds to $N_k = 62$, which is associated with the horizon crossing of the largest scales probed by the COBE satellite. Thus, by also having h_{end} we can derive h_0 from the above integral as being $h_0 \simeq 9.4 M_P/\sqrt{\xi}$. With the field value at horizon crossing, we can impose the normalization condition for the amplitude of the primordial power spectrum. Hence, importing the expression (1.35), we have:

$$\frac{V_*}{\epsilon_*} = 24\pi^2 M_P^4 A_S \simeq (0.027 M_P)^4 \ . \tag{2.24}$$

Recall that the subscript $*$ refers to the horizon crossing moment. Solving for V_*/ϵ_*, in terms of the h field, we get

$$\begin{aligned} \frac{V_*}{\epsilon_*} &\simeq \frac{3\lambda h_0^4}{16} \\ \implies \frac{3\lambda h_0^4}{16} &\simeq (0.027 M_P)^4 \ , \end{aligned} \tag{2.25}$$

where in the last equality we substituted (2.24). Inserting $h_{end} \simeq (4/3)^{1/4} M_P/\sqrt{\xi} \simeq 1.07 M_P/\sqrt{\xi}$ into (2.23) we get $h_0 \simeq \frac{4M_P}{3}\sqrt{\frac{N_k}{\xi}}$, which we can substitute back into (2.25) to get

$$\xi \simeq \sqrt{\frac{\lambda}{3}} \frac{N_k}{0.027^2} \simeq 49000\sqrt{\lambda} = 49000 \frac{m_H}{\sqrt{2}v} \ , \tag{2.26}$$

with $m_H = \sqrt{2\lambda} v$ being used in the last equality. As the authors in [Bezrukov and Shaposhnikov, 2008] noticed, concerning Higgs inflation, expression (2.26) relates the non-minimal coupling parameter, which is necessary to reproduce a viable inflationary expansion in the early Universe, to the Higgs mass, which is a well-measured parameter at low energies. Using $m_H \approx 125.35$ GeV and $v \approx 246$ GeV, we get $\xi \approx 1.8 \times 10^4$, supporting our $\xi \gg 1$ approximation. As far as the inflationary observables are concerned, we can readily compute the spectral index $n_S = 1 - 6\epsilon_* + 2\eta_* \approx 0.97$ and the tensor-to-scalar ratio $r = 16\epsilon_* \approx 0.0033$, for $N_k = 60$, corresponding to the scale $k = 0.002$ Mpc^{-1}. As an initial result, the above potential does in fact satisfies CMB requirements, as shown in Figures 2.3 and 2.4.

An objection that one might make regarding the suitability of the tree-level (classical) potential (2.21) for inflation is weather quantum corrections would be important at such high energies. In fact, the authors in [Bezrukov and Shaposhnikov, 2008] did consider this possibility. Whatever radiative corrections may arise, it is important that they do

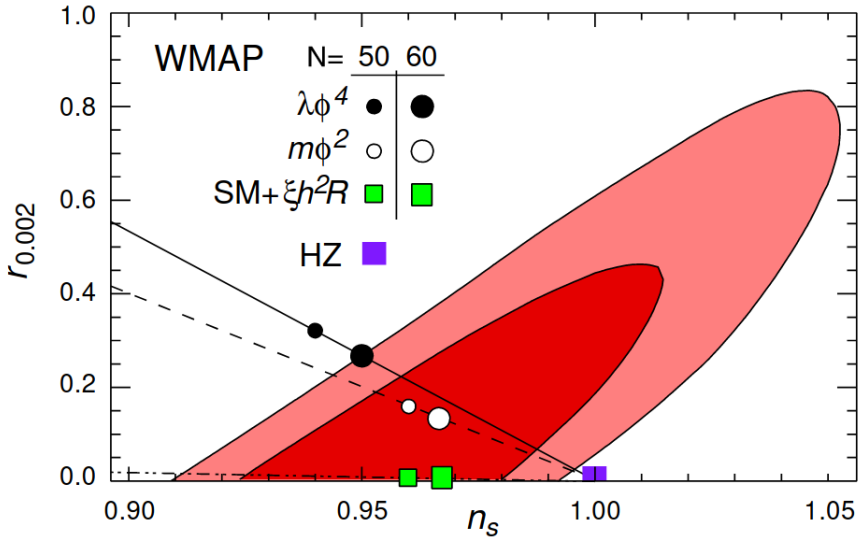

Figure 2.3: Contour intervals for the WMAP allowed region for n_S and r, assuming 50 and 60 e-folds [Bezrukov and Shaposhnikov, 2008].

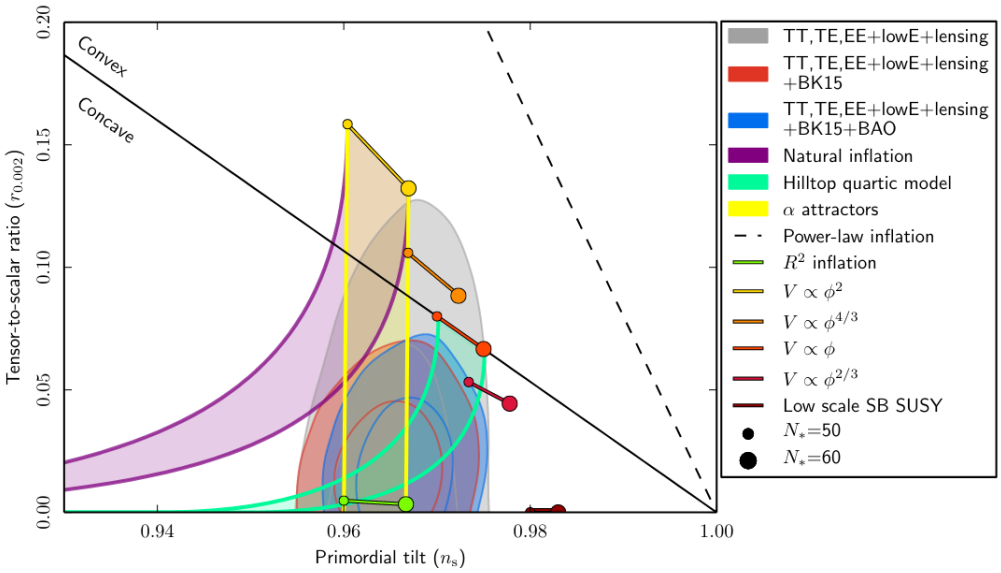

Figure 2.4: 68% and 95% Planck confidence levels in the $n_S - r$ plane, as well as the prediction for several inflationary models [Akrami et al., 2020].

not spoil the flatness of the potential during inflation, which would doom its success in reproducing the observed values of the spectral index and the tensor-to-scalar ratio. They also argue that the quantum corrections to the tree-level potential would come in two qualitatively different types. First, one can think about quantum gravity corrections. Those would be proportional to the energy density of the field, which is of the order $\rho_\chi \sim V_E(\chi)/M_P^4 \sim \lambda/\xi^2$. For large ξ required by observations, those terms are suppressed. Another kind of corrections are those induced by the coupling between the Higgs field and the other SM degrees of freedom[8]. In the one-loop approximation, these terms have the

[8]The authors in [Bezrukov and Shaposhnikov, 2008] also discuss corrections arising from the running

general structure[9]:

$$\Delta V(\chi) \sim \frac{m^4(\chi)}{64\pi^2} \ln \frac{m^2(\chi)}{\mu^2} \,, \tag{2.27}$$

where $m(\chi)$ is the mass of a given SM particle in the $\chi-$background and μ is a renormalization scale - to be discussed in the next Chapter. The masses of those fields get rescaled under the conformal transformation according to $\tilde{m}(\chi) = m(\chi)/\Omega(\chi) \sim 1/\sqrt{\xi}$, according to (2.14). Note that in the large-coupling regime ($\xi \gg 1$), the contributions in (2.27) become small and actually independent of χ. However, it was pointed out in [Barvinsky et al., 2008], that the true contributions of the corrected potential in the action are accompanied by a factor of $\sqrt{-\tilde{g}} = \Omega^4(\chi)\sqrt{-g}$. This has the effect that, if the corrections are computed in the Einstein frame, they are much weakly suppressed, proportional to the logarithm of the conformal factor. This raises the question of what frame is the most suited to compute the radiative corrections to the potential[10]. In this sense, the corrections can be computed according to prescription I (Einstein frame) or prescription II (Jordan frame) [Rodrigues et al., 2021]. It is argued in [Barvinsky et al., 2008] that prescription I is the most natural choice in order to relate the inflationary dynamics to low energy scales, since physical (atomic) clocks measure proper times that are related to the original Jordan frame metric. Nevertheless, without an ultraviolet completion of the SM coupled to gravity at hand, it is still difficult to judge from first principles which frame is more appropriate to compute quantum effects. In any case, since the quantum corrections during inflation ought to be small for the purpose of preserving the flatness of the potential, we expect that the results do not depend strongly on the choice of prescription. Although small, those radiative terms are useful to relate the inflationary requirements of the model to the electroweak observables measured at low energies, as we will discuss in the next Chapter.

of the non-minimal coupling ξ but those turn out to be negligible during inflation as well.

[9] We will indeed discuss similar one-loop corrections in the next chapter.

[10] Since the theory is not conformally invariant, the renormalization procedure yields results that possess a weak logarithm frame dependence.

Chapter 3

Non-Minimal Radiative Higgs Inflation

Having discussed the general non-minimal model of Higgs inflation in the previous Chapter, we now focus on a particular modification of the inflationary potential, featuring the inclusion of radiative corrections. In order to do that, we have to briefly discuss one of the greatest achievements of theoretical physics in the 20th century, the quantum theory of fields.

The development of quantum field theory (QFT) through the 1930s and 1940s was marked by a constant battle with infinities in the evaluation of amplitudes of several processes [Pais, 1986]. Those calculations, at higher orders in perturbation theory, were plagued by integrals that diverge when the internal momenta are too high. The salvation came when the pioneers of QFT admitted their ignorance: the theory should not be presumably valid to arbitrarily high energies. This reasoning motivated the advent of regularization schemes, such as the introduction of a cutoff in the calculation of divergent integrals, allowing the infinities to be identified[1]. Then, the renormalization program was able to remove such infinities by adding counterterms to the lagrangian, rendering the theory finite and predictive. That was, of course, a major step in establishing QFT as the framework for describing interactions among elementary particles.

3.1 The Effective Potential

One of the consequences of the renormalization procedure is that the constants of a renormalized theory are not actually constants. In order to relate renormalized amplitudes of processes occurring at different energy regimes, masses and coupling constants, for example, must also depend on the energy scale. The equations that govern the behaviour of the - now called - running couplings are collectively called Renormalization Group Equations (RGE) - see Section 3.4. Therefore, the Higgs potential showed in (2.3),

[1] Regularization schemes, such as Pauli-Villars regularization and dimensional regularization, allow one to identify the divergent terms in the calculation of loop diagrams of Green functions [Pascual and Tarrach, 1984].

which depends on the couplings μ and λ, must receive extra terms coming from the renormalization procedure, which we call quantum (or radiative) corrections.

One way to include such terms is to work with the effective potential, which includes in the tree-level (or zero-order) lagrangian quantum corrections up to a given order in perturbation theory. To leading order, the effective potential for a scalar field with potential $V(\phi)$ reads [Zee, 2003]

$$V_{\text{eff}}(\phi) = V(\phi) - \frac{i}{2}\int \frac{d^4k}{(2\pi)^4} \ln\left(\frac{k^2 - V''(\phi)}{k^2}\right) . \tag{3.1}$$

This is the Coleman-Weinberg potential [Coleman and Weinberg, 1973]. It encodes the first quantum corrections, also called one-loop order, to the potential energy of the background field ϕ, due to the emission and absorption of virtual particles [Sher, 1989]. The integral in (3.1) is an example of a divergent integral, mentioned earlier. It turns out that it has a quadratic and a logarithmic divergence when the integrated momenta go to arbitrarily large values. Thus, we include two counterterms and integrate up to a cutoff Λ:

$$\begin{aligned} V_{\text{eff}}(\phi) &= V(\phi) - \frac{i}{2}\int^{\Lambda} \frac{d^4k}{(2\pi)^4} \ln\left(\frac{-k^2 + V''(\phi)}{-k^2}\right) + B\phi^2 + C\phi^4 \\ &= V(\phi) + \frac{\Lambda^2}{32\pi^2}V''(\phi) - \frac{1}{64\pi^2}[V''(\phi)]^2 \ln\left[\frac{\Lambda^2}{V''(\phi)}\right] + B\phi^2 + C\phi^4 . \end{aligned} \tag{3.2}$$

Hence, if $V(\phi)$ is at most a fourth order polynomial, $V''(\phi)$ and $[V''(\phi)]^2$ are, respectively, quadratic and quartic in ϕ, meaning that they are precisely canceled by the two counterterms. Therefore, we work with the massless scalar potential (2.3), given that, at the inflationary regime of interest, at high field values $h \gg v$, we can safely ignore the mass term. Thus, substituting $V(\phi) = \frac{\lambda}{4}\phi^4$ in the above expression, yields

$$V_{\text{eff}}(\phi) = \frac{\lambda}{4}\phi^4 + \frac{3\Lambda^2}{32\pi^2}\lambda\phi^2 + \frac{3\lambda^2}{128\pi^2}\phi^4 \ln\left(\frac{\phi^2}{\Lambda^2}\right) + B\phi^2 + C\phi^4 . \tag{3.3}$$

Note that the second and third terms precisely contain the quadratic and logarithmic divergence when Λ is taken to infinity. They can be removed by carefully fixing the coefficients B and C, which amounts to imposing renormalization conditions on the effective potential. In the original massless potential, $V(\phi) = \frac{\lambda}{4}\phi^4$, we had $\frac{d^2V}{d\phi^2}|_{\phi=0} = 0$. In order to keep with a (renormalized) massless theory, we have to impose $\frac{d^2V_{\text{eff}}}{d\phi^2}|_{\phi=0} = 0$. This fixes the first constant $B = -\frac{3\Lambda^2}{32\pi^2}\lambda$. Accordingly, in the classical potential, the quartic coupling is given by $\frac{d^4V}{d\phi^4} = 6\lambda$. However, since $\frac{d^4V_{\text{eff}}}{d\phi^4}$ depends on $\ln\phi$, we cannot evaluate it at $\phi = 0$. Thus, we set the second renormalization condition at an arbitrary high-energy

scale μ, as $\frac{d^4V_{\text{eff}}}{d\phi^4}|_{\phi=\mu} = 6\lambda(\mu)$, where $\lambda(\mu)$ is the renormalized quartic coupling, given by

$$\frac{d^4V_{\text{eff}}}{d\phi^4}\Big|_{\phi=\mu} = 6\lambda - \frac{9\lambda^2}{16\pi^2}\ln\left(\frac{\Lambda^2}{\mu^2}\right) + \frac{75\lambda^2}{32\pi^2} + 24C = 6\lambda(\mu)\ . \tag{3.4}$$

From (3.4), we can read off the second counterterm as $C = \frac{1}{4}[\lambda(\mu) - \lambda] + \frac{3\lambda^2}{128\pi^2}\left[\ln\left(\frac{\Lambda^2}{\mu^2}\right) - \frac{25}{6}\right]$. Substituting B and C back into (3.3) we obtain

$$V_{\text{eff}}(\phi) = \frac{\lambda}{4}\phi^4 + \frac{3\lambda^2}{128\pi^2}\left[\ln\left(\frac{\phi^2}{\mu^2}\right) - \frac{25}{6}\right]\phi^4\ , \tag{3.5}$$

where the quartic coupling is now renormalized at a given scale $\lambda(\mu)$. We also highlight that, as expected, the effective potential has lost its dependence on the cutoff Λ.

Although it seems that the effective potential has a dependence on the scale μ, we can absorb it in the renormalized coupling $\lambda(\mu)$. Therefore, if we had chosen a different renormalization scale μ', we would have obtained the same potential with a new coupling $\lambda(\mu')$. In fact, we can express the variation of the coupling with the scale by demanding that $\mu\frac{dV_{\text{eff}}}{d\mu} = 0$, which gives [Zee, 2003]

$$\mu\frac{d\lambda(\mu)}{d\mu} = \frac{3\lambda^2(\mu)}{16\pi^2} = \beta_\lambda(\mu)\ , \tag{3.6}$$

with β_λ being the quartic coupling's beta-function, which measures the variation of the coupling with the renormalization scale. Substituting β_λ back into (3.5) and performing the field redefinition $\ln(\frac{h^2}{\mu^2}) = \ln\frac{\phi^2}{\mu^2} - \frac{25}{6}$ to remove the constant terms in the logarithm, we get

$$V_{\text{eff}}(h) = \frac{\lambda}{4}h^4 + \frac{\beta_\lambda}{4}h^4\ln\left(\frac{h}{\mu}\right)\ . \tag{3.7}$$

The potential (3.7) was derived by considering a simple scalar field. In the context of the Higgs in the SM, one has to account for the coupling of the Higgs with other particle species, which makes the renormalization procedure somewhat more involved. Nonetheless, the resulting effective potential recovers the general structure of (3.5), with the effective coupling $\lambda(\mu)$ encoding the contributions from the relevant running couplings of the electroweak model [Sher, 1989]. Also, it is mentioned in [Rodrigues et al., 2021] and references therein, that the Higgs quartic coupling and its beta-function holds only a weak dependence on the renormalization scale μ at high energies. Thus, we can use the expression (3.7) as an approximation for the Higgs effective potential:

$$V_{\text{eff}}(h) \approx \frac{\lambda}{4}h^4\left(1 + a'\ln\frac{h}{M_P}\right)\ , \tag{3.8}$$

where M_P is the high energy scale around which the approximation (3.8) is valid. An important parameter in our analysis is $a' \equiv \frac{\beta_\lambda}{\lambda}$, since it quantifies the deviation from the tree-level potential. Therefore, the above expression can be interpreted as a generalization of the quartic potential used in the non-minimal model of (2.11), where radiative corrections, computed in the Jordan frame, are included.

3.2 Slow-Roll Analysis

As usual in non-minimal models of inflation, we apply the set of transformations (2.12) and (2.16) in order to check the suitability of the potential (3.9) as a model for single-field slow-roll inflation. Therefore, the effective potential in the Einstein frame reads

$$V_{\text{eff}}(\chi) \approx \frac{\lambda M_P^4}{4\xi^2}\left(1 - e^{-\sqrt{\frac{2}{3}}\frac{\chi}{M_P}}\right)^2\left(1 + a' \ln\sqrt{\frac{1}{\xi}e^{\sqrt{\frac{2}{3}}\frac{\chi}{M_P}} - \frac{1}{\xi}}\right) . \tag{3.9}$$

In a similar fashion to what was done in the last Chapter with the standard non-minimal Higgs inflation, we can compute the spectral index and tensor to scalar ratio for the potential (3.9) according to the expressions showed in (1.35). As always, note that the slow-roll parameters are evaluated at the horizon crossing moment which is determined once the number of e-folds during inflation is specified. Extending the results of [Rodrigues et al., 2021], we perform the calculation for $N_k = 50, 55, 60$. The results are presented in Figure (3.1).

The curves represent a range of the radiative parameter from -0.1 (lower limit) to 1.0 (upper limit)[2], for each number of e-folds. Note that there is a significant dependence of the inflationary predictions with the amount of expansion during inflation, achieving compatibility with the Planck result[3]. We will indeed perform a more detailed analysis for a wider range of e-folds in the next Section. It is also important to mention that the results obtained for the prediction of inflationary parameters are highly independent of the parameter ξ, once the strong-coupling regime is assumed.

3.3 Varying e-fold Number and Reheating Analysis

The number of e-folds during inflation is not a free parameter entirely, as it is tied to the subsequent evolution of the Universe, given its association with the horizon exit of relevant cosmological scales. As mentioned in Chapter 1, the relevant scales probed by Planck seem to correspond to an interval of 50-60 e-folds, which guides our range of

[2]The values of a' varying between [-0.010, 0.053], [-0.020, 0.036] and [-0.027, 0.023], corresponding to $N_k = 50$, 55 and 60, respectively, are in agreement with the 95% C.L. Planck result [Aghanim et al., 2020a].

[3]This agreement relies on the slow-roll approximations for the inflationary parameters and the phenomenological power-law expansion of the primordial power spectrum.

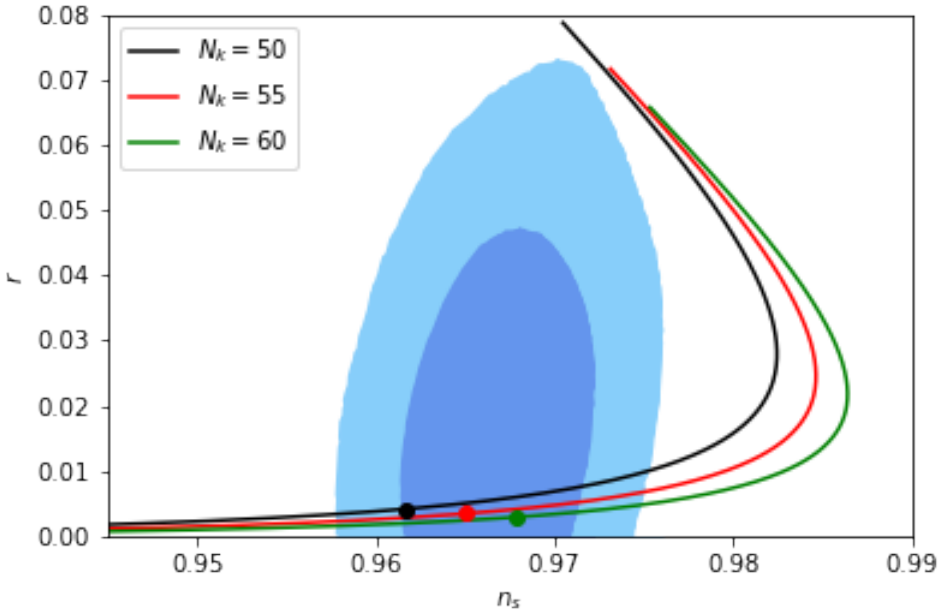

Figure 3.1: n_s vs. r for $N_k = 50, 55$ & 60. The points in each curve indicate the parameters for a null resultant of the radiative corrections ($a' = 0$). The blue areas show the favored regions by *Planck 2018*, with 68% and 95% confidence level (Planck TT, TE, EE + lowE + lensing + BK15 + BAO data set) [Aghanim et al., 2020a, Rodrigues et al., 2023].

exploration of the parameter N_k, associated with the horizon exit of the chosen pivot scale $k = 0.05$ Mpc^{-1}.

In order to constrain the model with cosmological data, we develop the methodology exploited in [Rodrigues et al., 2021], which was also used in [Rodrigues et al., 2023]. Thus, we consider the standard values for most of the cosmological parameters, namely, the the physical baryon density, ω_b, the physical cold dark matter density, ω_c, the optical depth, τ, and the angular diameter distance at decoupling, θ. However, we do not consider the usual parametrization of the primordial power spectrum, in terms of the amplitude of scalar perturbations, A_S, and the spectral index, n_S, even though, as we have seen in Chapter 1, they are closely related to the inflationary potential in the slow-roll approximation. Instead, we modify the Boltzmann solver Code for Anisotropies in the Microwave Background (CAMB), according to the specifications of ModeCode, which allows the computation of the primordial power spectrum directly in terms of the inflationary potential, without needing to resort to the power-law parametrization. This has the advantage of replacing the usual cosmological parameters A_S and n_S with the parameters of the potential ξ and a', where the latter is free to vary[4].

In addition, we perform a MCMC analysis to estimate the parameters of the model

[4]Since the results are highly independent of ξ once the strong-coupling regime is assumed, we choose $\xi = 1000$ for the numerical calculation.

with the CosmoMC package and a combination of early- and late-time data[5]. Since we are interested in relating our results with the electroweak scale via an estimation of the top quark mass (see Section 3.4), the main focus of our analysis is in the radiative parameter a'. Note that the potential (3.9) is dependent on the parameters λ, ξ and a'. Therefore, we can use the expression for the measured amplitude of primordial perturbations (1.35) as a constraint equation in order to express $\lambda(\xi, a')$. Thus, by fixing the non-minimal coupling parameter, our analysis returns an unique value for a'. Figure (3.2) shows the derived constraints on the most significant parameters of our analysis for N_k in the $50-60$ range. In order to narrow our range of exploration of the parameter N_k, we can perform

	a'	$r_{0.02}$	H_0	σ_8
N_k=50	0.179 ± 0.072	0.032 ± 0.013	68.82 ± 0.38	0.841 ± 0.005
N_k=52	0.040 ± 0.015	0.007 ± 0.002	68.31 ± 0.41	0.835 ± 0.005
N_k=54	0.011 ± 0.014	0.004 ± 0.001	67.71 ± 0.45	0.817 ± 0.003
N_k=54.5	0.009 ± 0.013	0.004 ± 0.001	67.68 ± 0.43	0.811 ± 0.003
N_k=55	0.010 ± 0.013	0.004 ± 0.001	67.71 ± 0.44	0.804 ± 0.003
N_k=56	0.022 ± 0.015	0.005 ± 0.001	67.94 ± 0.45	0.793 ± 0.003
N_k=58	0.283 ± 0.169	0.044 ± 0.019	68.37 ± 0.39	0.779 ± 0.004
N_k=60	0.243 ± 0.088	0.042 ± 0.015	68.46 ± 0.38	0.766 ± 0.005

Figure 3.2: Constraints for fixed N_k at 68% C.L. using the Planck $TT, TE, EE + lowE + lensing + BICEP2/Keck + BAO + Pantheon$ combination [Rodrigues et al., 2023].

a general reheating analysis with the tools we developed in Section 1.1.3. At first, we can analytically explore the behavior of the potential (3.9) at different field values, obtained when the inflaton evolves from deep in the inflationary epoch into the reheating stage. To this end, we closely follow the steps developed in [Bezrukov et al., 2009]. First, note that for field values $\chi < \chi_e \sim M_P$, immediately after the end of inflation, we can expand the exponentials in (3.9) according to: $e^{\sqrt{\frac{2}{3}}\frac{\chi}{M_P}} \approx 1 + \sqrt{\frac{2}{3}}\frac{\chi}{M_P}$. Under this approximation, we can rewrite the potential as

$$V_E(\chi) \approx \frac{\lambda M_P^2}{6\xi^2}\chi^2\left[1 + \frac{a'}{4}\ln\left(\frac{2}{3\xi}\frac{\chi^2}{M_P^2}\right)\right] . \tag{3.10}$$

Therefore, apart from a small logarithmic correction proportional to the radiative parameter, the potential is approximately quadratic right at the end of the inflationary regime. As discussed in Section 1.1.3, this is characteristic of the preheating stage, where strong coherent oscillations of the inflaton condensate are expected to happen. Also, we previously pointed out that a polynomial potential of the type $V(\chi) \propto \chi^n$ is associated with an effective equation of state parameter $w = \frac{n-2}{n+2}$. Thus, the quasi-quadratic potential

[5] We use the CMB Planck (2018) likelihood [Aghanim et al., 2020b], using Plik temperature power spectrum, TT, and HFI polarization EE likelihood at $\ell \leqslant 29$; BICEP2 and Keck Array experiments B-mode polarization data [Ade et al., 2018]; BAO measurements from 6dFGS [Beutler et al., 2011], SDSS-MGS [Ross et al., 2015], and BOSS DR12 [Alam et al., 2017] surveys, and the Pantheon sample of Type Ia supernovae [Scolnic et al., 2018].

after expansion induces an expansion of the cosmos as if it is dominated by a matter-like fluid. Let us assign to this initial state a duration of N_1 e-folds, with equation of state parameter $w_1 \approx 0$.

To proceed for smaller field values, note that the transformation law between the scalar fields in the Jordan and Einstein frames, (2.16), can be rewritten in the large-coupling approximation ($\xi \gg 1$) as

$$\frac{d\chi}{dh} \approx \sqrt{\frac{1+6\xi^2\frac{h^2}{M_P^2}}{(1+\xi\frac{h^2}{M_P^2})^2}} \approx \sqrt{\frac{1+\frac{h^2}{h_{cr}^2}}{(1+\frac{2}{3\xi}\frac{h^2}{h_{cr}^2})^2}}\,, \tag{3.11}$$

where we have defined $h_{cr} \equiv \sqrt{\frac{2}{3}}\frac{M_P}{\xi}$. For $h > h_{cr}$, we recover the $\chi(h)$ expression of (2.19) by direct integration of (3.11). For $h < h_{cr}$, we obtain the simple relation $d\chi/dh \approx 1$, which implies that $h \sim \chi$ and we can use (2.17) to write

$$\begin{aligned} V_E(\chi) &= \frac{V_J(h)}{\Omega^4(h)} \\ &= \frac{1}{(1+\xi\frac{h^2}{M_P^2})^2}\frac{\lambda}{4}h^4\left[1+\frac{a'}{2}\ln\left(\frac{h}{M_P}\right)^2\right] \\ &= \frac{1}{(1+\frac{2}{3\xi}\frac{h^2}{h_{cr}^2})^2}\frac{\lambda}{4}h^4\left[1+\frac{a'}{2}\ln\left(\frac{h}{M_P}\right)^2\right] \\ &\approx \frac{\lambda}{4}\chi^4\left[1+\frac{a'}{2}\ln\left(\frac{\chi}{M_P}\right)^2\right]\,. \end{aligned} \tag{3.12}$$

In the last step, we again used the $h < h_{cr}$ and $h \sim \chi$ approximations. Note that the potential becomes approximately fourth-order in the field χ, associated with a Universe expansion dominated by a radiation-like fluid component. To this later stage, we assign a duration of N_2 e-folds with equation of state parameter $w_2 \approx 1/3$.

Therefore, we can summarize the different behaviors for the potential for distinct field regimes according to:

$$V_E(\chi) \approx \begin{cases} \frac{\lambda M_P^4}{4\xi^2}\left(1-e^{-\sqrt{\frac{2}{3}}\frac{\chi}{M_P}}\right)^2\left(1+a'\ln\sqrt{\frac{1}{\xi}e^{\sqrt{\frac{2}{3}}\frac{\chi}{M_P}}-\frac{1}{\xi}}\right), & \chi > \chi_e \\ \frac{\lambda M_P^2}{6\xi^2}\chi^2\left[1+\frac{a'}{4}\ln\left(\frac{2}{3\xi}\frac{\chi^2}{M_P^2}\right)\right], & \chi_{cr} < \chi < \chi_e \\ \frac{\lambda}{4}\chi^4\left[1+\frac{a'}{2}\ln\left(\frac{\chi}{M_P}\right)^2\right], & \chi < \chi_{cr}\,, \end{cases} \tag{3.13}$$

where $\chi_e \sim M_P$ and $\chi_{cr} \equiv \sqrt{\frac{2}{3}}\frac{M_P}{\xi}$. Again, we assign to each regime of the potential an effective equation of state parameter of $w_{inf} = -1$, $w_1 \approx 0$ and $w_2 \approx 1/3$.

Thus, we have the picture of a reheating stage divided into a matter- and radiation-like

expansion periods. Therefore, we have to slightly modify the matching equation (1.44) in order to replace the unknown global reheating equation of state parameter w_{reh} with the known $w_1 = 0$ and $w_2 = 1/3$. To this end, we follow the procedure outlined in [Gong et al., 2015]. The splitting of the number of e-folds during reheating into $N_{reh} = N_1 + N_2$ has the effect of modifying the expression (1.38) according to:

$$\ln\left(\frac{k}{a_0 H_0}\right) = -N_k - N_1 - N_2 - N_{RD} + \ln\left(\frac{a_{eq}H_{eq}}{a_0 H_0}\right) + \ln\left(\frac{H_k}{H_{eq}}\right) . \tag{3.14}$$

Analogously to what was done in Section 1.1.3, the e-fold numbers for the first and second reheating stage can be expressed as $N_1 = \frac{1}{3(1+w_1)} \ln\left(\frac{\rho_{end}}{\rho_{cr}}\right)$ and $N_2 = \frac{1}{3(1+w_2)} \ln\left(\frac{\rho_{cr}}{\rho_{reh}}\right)$, where ρ_{cr} is the energy density of the cosmic fluid at the transition time between matter and radiation dominance during reheating, associated with the field value χ_{cr}. We can further manipulate N_2 to find an useful expression:

$$\begin{aligned} N_2 &= \frac{1}{3(1+w_2)} \ln\left(\frac{\rho_{cr}}{\rho_{reh}}\right) \\ &= \frac{1}{3(1+w_2)} \ln\left(\frac{\rho_{cr}}{\rho_{end}}\frac{\rho_{end}}{\rho_{reh}}\right) \\ &= \frac{1}{3(1+w_2)} \left[\ln\left(\frac{\rho_{cr}}{\rho_{end}}\right) + \ln\left(\frac{\rho_{end}}{\rho_{reh}}\right)\right] . \end{aligned} \tag{3.15}$$

Therefore, the combination $-N_1 - N_2$ appearing in (3.14) can be rewritten as

$$\begin{aligned} -N_1 - N_2 &= \frac{1}{3(1+w_1)} \ln\left(\frac{\rho_{cr}}{\rho_{end}}\right) - \frac{1}{3(1+w_2)} \left[\ln\left(\frac{\rho_{cr}}{\rho_{end}}\right) + \ln\left(\frac{\rho_{end}}{\rho_{reh}}\right)\right] \\ &= \left[\frac{1}{3(1+w_1)} - \frac{1}{3(1+w_2)}\right] \ln\left(\frac{\rho_{cr}}{\rho_{end}}\right) - \frac{1}{3(1+w_2)} \ln\left(\frac{\rho_{end}}{\rho_{reh}}\right) . \end{aligned} \tag{3.16}$$

Note that the last term in (3.16) is precisely the definition of N_{reh} in (1.39) with w_{reh} replaced by w_2. Hence, if we substitute (3.16) into (3.14) we arrive at

$$\begin{aligned} \ln\left(\frac{k}{a_0 H_0}\right) = &- N_k - N_{reh}\big|_{w_2} - N_{RD} + \ln\left(\frac{a_{eq}H_{eq}}{a_0 H_0}\right) + \ln\left(\frac{H_k}{H_{eq}}\right) \\ &+ \left[\frac{1}{3(1+w_1)} - \frac{1}{3(1+w_2)}\right] \ln\left(\frac{\rho_{cr}}{\rho_{end}}\right) . \end{aligned} \tag{3.17}$$

This last expression is exactly the matching equation (1.38) with $w_{reh} \to w_2$ and an additional term. We can perform the same steps of Section 1.1.3 to derive the analog of

equation (1.44):

$$N_k = \frac{-1+3w_2}{4}N_{reh} - \ln\left(\frac{V_{end}^{1/4}}{H_k}\right) + 61.55 + \left[\frac{1}{3(1+w_1)} - \frac{1}{3(1+w_2)}\right]\ln\left(\frac{\rho_{cr}}{\rho_{end}}\right)$$
$$= \frac{1-3w_2}{12(1+w_2)}\ln\left(\frac{\rho_{reh}}{\rho_{end}}\right) - \ln\left(\frac{V_{end}^{1/4}}{H_k}\right) + 61.55 + \left[\frac{1}{3(1+w_1)} - \frac{1}{3(1+w_2)}\right]\ln\left(\frac{\rho_{cr}}{\rho_{end}}\right) , \tag{3.18}$$

where in the last equality we used $N_{reh} = \frac{1}{3(1+w_2)}\ln\left(\frac{\rho_{end}}{\rho_{reh}}\right)$.

Now, substituting the equation of state parameters $w_1 = 0$ and $w_2 = 1/3$, and using $N_1 = \frac{1}{3}\ln\left(\frac{\rho_{end}}{\rho_{cr}}\right)$, we finally arrive at

$$N_k = -\frac{1}{4}N_1 - \ln\left(\frac{V_{end}^{1/4}(a')}{\sqrt{V_*(a')/3}}\right) + 61.55 \, . \tag{3.19}$$

We have also used the background equation to approximate $H_k \sim \sqrt{V_*/3}$, valid at the horizon crossing moment during inflation, and we highlight the a' dependence of the potential.

Let us now pause for a moment to interpret this last result. Based on the behavior of the scalar field potential at different field regimes, we have effectively exchanged the unknown expansion of the Universe during reheating to an initial matter-dominated expansion, parameterized by the e-fold number N_1. The price to pay is that the later radiation-dominated stage of reheating gets confused with the actual onset of the Hot Big Bang evolution, which is also dominated by radiation. For our purposes of constraining the number of e-folds during inflation, this distinction will turn out to be harmless.

Thus, although the details of the physical processes that took place during the reheating epoch are highly obscure, one can attempt to constrain this period observationally. With equation (3.19), we can relate the inflationary e-fold number probed in our analysis with the duration of the initial matter-dominated reheating stage, quantified by N_1. A plot of (3.19), with each value of a' coming from a Monte Carlo Markov Chain (MCMC) analysis, is made in Figure (3.3).

Note that for a number of e-folds during inflation of ~ 56 or greater, N_1 would have to be negative in order to satisfy the matching condition (3.19), implying in a contraction of the Universe during the initial matter-dominated period of reheating. Therefore, we regard those values as non-physical. Hence, in the context of the non-minimal Higgs inflation scenario, we infer a maximum number of inflationary e-folds that results in an instantaneous transition to the radiation-dominated expansion. According to Table 1, $N_k = 56$ is associated with a radiative parameter of approximately $a' = 0.022 \pm 0.015$. We will explore further consequences of this value of the inflationary e-fold number in the

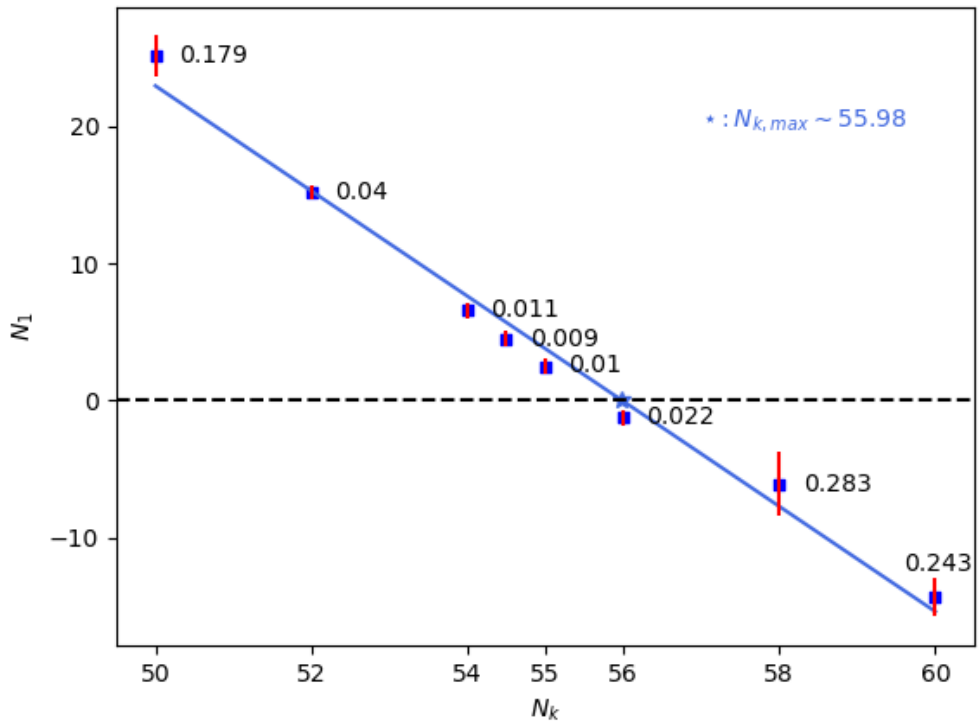

Figure 3.3: N_k vs. N_1 for each inflationary number of e-folds taken into consideration. N_1 is given by the matching equation (3.19), with a' coming from the MCMC analysis (highlighted beside each point). Through a linear regression between the points (solid blue line), we estimate a maximum number N_k - where the transition to a radiation-dominated Universe happens instantaneously [Rodrigues et al., 2023].

following Sections.

3.4 Constraints on the Top Quark mass

We are now in position to link our results to the electroweak scale. This can be interpreted as a consistency test for the inflationary constraints on the Higgs potential, namely on the radiative parameter a'. The chosen quantity for comparison will be the top quark pole mass, due to the inherent uncertainties in its Monte Carlo mass reconstruction [Butenschoen et al., 2016]. Then, we can compare our assessment with the latest inferred values from low-energy physics.

Our method's main tool will be the Renormalization Group Equations [Sher, 1989]. As briefly discussed in the beginning of this Chapter, those equations are intrinsically connected with the non-dependence of physical quantities with energy scales, which, in turn, make the parameters of a given theory - such as masses and coupling constants - functions of energy. We can start our quantitative analysis by considering a generalization of the potential (3.5), where the Higgs effective potential now depends on several other

couplings λ_i as well as on the renormalization scale: $V_{\rm eff}(h, \lambda_i, \mu)$. Thus, applying the chain rule to $\mu \frac{dV_{\rm eff}}{d\mu} = 0$, we get

$$\left(\mu\frac{\partial}{\partial\mu} + \beta_i\frac{\partial}{\partial\lambda_i} - \gamma\frac{\partial}{\partial h}\right) V_{eff} = 0 \,, \tag{3.20}$$

where $\beta_i \equiv \mu\frac{\partial\lambda_i}{\partial\mu}$ are the β-functions for the relevant coupling constants and $\gamma \equiv -\frac{\mu}{h}\frac{dh}{d\mu}$ the Higgs field anomalous dimension.

The set of partial differential coupled equations (3.20) determine the flow of the parameters of the potential V_{eff} as a function of the renormalization scale μ, according to the symmetries and particle content of the theory. For the SM, we are particularly interested in the flow of the Higgs quartic coupling λ, the top quark Yukawa coupling y_t, the electroweak g and g' gauge couplings and the strong g_S gauge coupling[6]. Naturally, a set of differential equations for the relevant parameters require a set of contour conditions. Following the standard approach, we fix the gauge couplings g and g' to its central values at the electroweak scale. Therefore, according to [Zyla et al., 2020], we obtain their values in the $\overline{\rm MS}$ renormalization scheme as being:

$$\begin{aligned} g(\mu = m_Z) &= \sqrt{4\pi\alpha_{em}\sin^2\theta_W} = 0.651784 \\ g'(\mu = m_Z) &= \sqrt{4\pi\alpha_{em}\cos^2\theta_W} = 0.35744 \,, \end{aligned} \tag{3.21}$$

with $\alpha_{em} = 1/137$ being the electromagnetic fine-structure constant. As for λ, y_t, and g_S, higher order threshold corrections are needed at the weak scale, given the magnitude of QCD and top Yukawa interactions [Rodrigues et al., 2021]. We can make use of the interpolating formulas obtained in [Buttazzo et al., 2013]:

$$\begin{aligned} \lambda(\mu = m_t) &= 0.12604 + 0.00206\left(\frac{m_H}{\rm GeV} - 125.15\right) - 0.00004\left(\frac{m_t}{\rm GeV} - 173.34\right) \\ y_t(\mu = m_t) &= 0.93690 + 0.00556\left(\frac{m_t}{\rm GeV} - 173.34\right) - 0.00042\left(\frac{m_H}{\rm GeV} - 125.15\right) \\ g_S(\mu = m_t) &= 1.1666 + 0.00314\frac{\alpha_S(m_Z) - 0.1184}{0.0007} - 0.00046\left(\frac{m_t}{\rm GeV} - 173.34\right) \,, \end{aligned} \tag{3.22}$$

where α_S is the $\overline{\rm MS}$ strong coupling[7].

With the current global fit of the electroweak precision data as contour conditions and the two-loop β-functions (Appendix A of [Rodrigues et al., 2021]), we can solve the set of RGEs. Note that the Higgs and top quark pole masses appear as input parameters of the contour conditions. For the Higgs boson, we opt to fix its pole mass to the central value

[6] In principle, we would also need to include the flow of the non-minimal parameter ξ. However, as was the case for the slow-roll analysis, our main results will only show a mild dependence to a specific value of ξ, once the large-coupling regime is assumed. Nevertheless, we will specify the value of ξ when needed.

[7] Per [Zyla et al., 2020], we set its central value to $\alpha_S = 0.1179 \pm 0.0010$.

obtained in [Zyla et al., 2020] of $m_H = 125.10 \pm 0.14$ GeV. On the other hand, we leave the top quark pole mass as a free parameter, which shall be determined based on our cosmological estimation of the radiative parameter a'. Our analysis proceeds as follows. Note that, once we have solved the RGE for a given value of m_t, we will have the values at $\mu = M_P$ of both λ and β_λ. Since, per definition, $a' = \beta_\lambda/\lambda$, we can tune the top quark mass m_t in order to obtain $\beta_\lambda(M_P)$ and $\lambda(M_P)$ which, in turn, yields an a' parameter consistent with the values given in the cosmological MCMC analysis - see Table (3.2). In [Rodrigues et al., 2021], the authors performed a thorough investigation for $N_k = 55$, where the main results are plotted in Figure (3.4). In this occasion, it was found that, in order to reproduce the value of $a'(M_P)$ consistent with the MCMC analysis, one must impose and upper limit of $m_t \leqslant 170.222$ GeV in the solution of the RGEs.

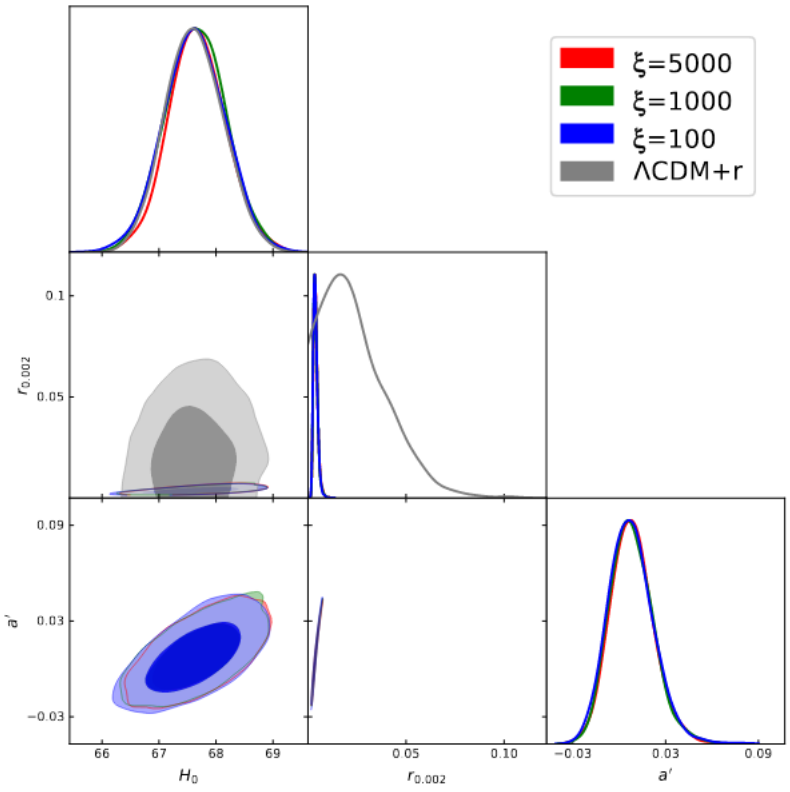

Figure 3.4: Posterior distribution of the MCMC analysis developed in [Rodrigues et al., 2021] for $N_k = 55$. Note that the constraints on the cosmological parameters overlap for each value of the non-minimal coupling ξ.

In our work [Rodrigues et al., 2023], we had the opportunity to perform a similar investigation for a wider range of the inflationary e-fold number, while keeping in mind the upper limit of $N_k \sim 56$, derived from the reheating considerations. In this case, where the transition to the radiation dominated epoch happens instantaneously, we find $m_t \leqslant 170.44$ GeV, in order to reproduce the a' value cited earlier.

The comparison with electroweak measurements is based on two distinct methodologies. One class of constraints on the top quark mass are obtained from the kinematic

reconstruction of $t\bar{t}$ events, where m_t is employed in a Monte-Carlo generator in order to fit the data [Abazov et al., 2004, Abe et al., 1994]. From [Workman and Others, 2022], the average value for the top quark mass is set to $m_t = 172.69 \pm 0.30$ GeV, obtained from LHC and Tevatron data. If contrasted with the limit on m_t from our cosmological analysis, this represents a significant discrepancy of $\approx 7.5\sigma$.

Instead, one may consider the inference of the top quark pole mass on measurements of the cross-section of the top quark production, since the theoretical computation of $\sigma(t\bar{t})$ is explicitly performed in a particular renormalization scheme (e.g., MS) [Langenfeld et al., 2009]. In this case, the average value, obtained from the Tevatron and LHC runs, is $m_t = 172.5 \pm 0.7$ GeV [Workman and Others, 2022], lowering the discrepancy with our cosmological estimate to $\approx 3\sigma$. More recently, the CMS collaboration reported $m_t = 170.5 \pm 0.8$ GeV, obtained from the differential cross-section of top production [Sirunyan et al., 2020]. Such result perfectly agrees with the results of our cosmological analysis of Higgs Inflation.

3.5 Breaking the $H_0 - \sigma_8$ Correlation

In Chapter 1, we highlighted some ongoing tensions involving important parameters of ΛCDM Cosmology, in light of distinct early- and late-time cosmological surveys. Perhaps the most important discrepancy between observational results is the disagreement on the Hubble parameter H_0 inferred from the CMB anisotropies and its measured value from SNIa redshift-distance relation. Also, the clustering parameter on the $8h^{-1}$ Mpc scale, σ_8, based on lensing estimation by the Kilo-Degree Survey (KiDS-1000) is currently constrained to $\sigma_8 = 0.766^{+0.024}_{-0.021}$ [Asgari et al., 2021], which is higher than expected from CMB measurements. In addition to the two tensions, these parameters are also correlated, as discussed in Section 1.2.1. Thus, by increasing the CMB inferred value for H_0, for the sake of lowering the tension with local measurements, we end up increasing the estimation for σ_8, worsening its agreement with local data.

We can ask ourselves how the Hubble constant and the clustering parameter are reproduced in our analysis as a function of the inflationary e-fold number. The posterior distributions are shown in Figure 3.5.

Note from the figure and Table 3.2 that both H_0 and σ_8 decrease from $N_k = 50$ until the turning point at $N_k = 54.5$. However, from that e-fold number up to $N_k = 60$, σ_8 continues to show smaller values while H_0 increases. Thus, for $N_k > 54.5$, the model breaks the correlation between the Hubble constant and the clustering parameter, as also shown in Figure 3.5. In particular, for our limiting case of $N_k = 56$, corresponding to an instantaneous transition to the radiation-dominated epoch, the analysis returns $H_0 = 67.94 \pm 0.45$ Km s^{-1} Mpc^{-1}, reducing the Hubble constant tension to $\approx 3\sigma$ from SNIa measurements [Riess et al., 2022]. Also, the constrained value for the clustering

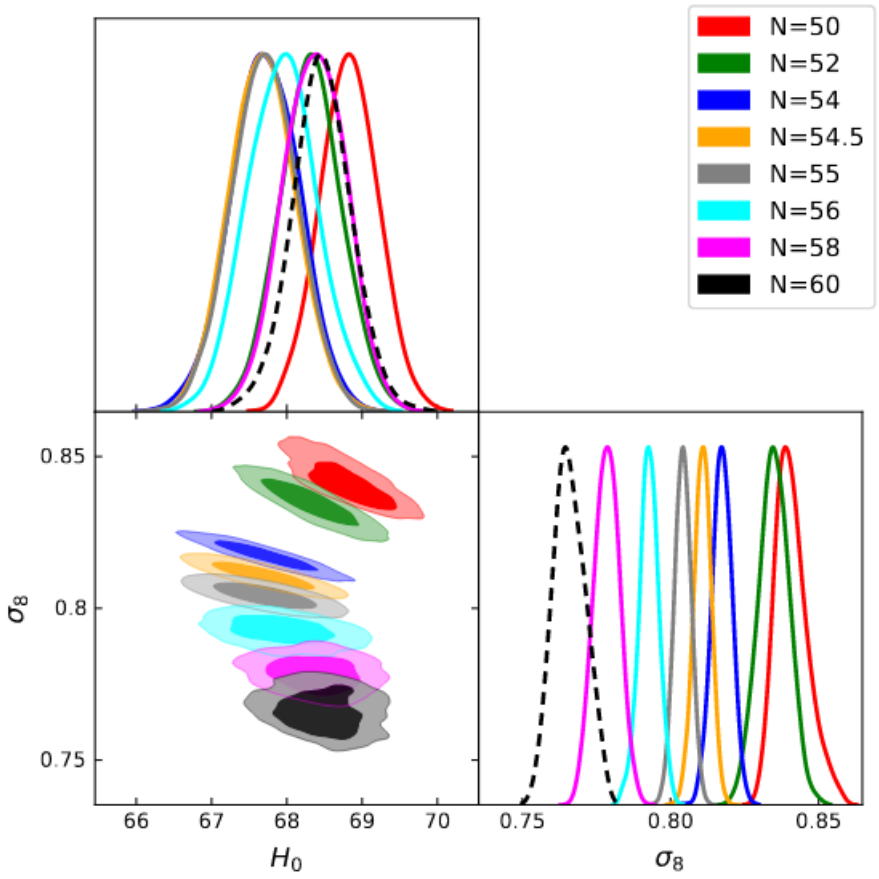

Figure 3.5: Confidence levels and posterior distributions for the H_0 and σ_8 parameters using the joint data set CMB Planck (2018) + BICEP2 and Keck Array + BAO + Pantheon SNe Ia sample and considering several values of N_k [Rodrigues et al., 2023].

parameter is at $\sigma_8 = 0.793 \pm 0.003$, which is in full agreement with KiDS-1000 results [Asgari et al., 2021].

Chapter 4

Conclusions

We started our discussion in Chapter 1 with several aspects of the standard description of Cosmology, based on the General Theory of Relativity and the Cosmological Principle. We have seen that the Hot Big Bang model, formulated in terms of a FLRW spacetime, does not provide a satisfactory explanation for the near homogeneity of large-scale structure, as well as its superhorizon correlations, primarily manifested in the temperature distribution of the CMB. Thus, one is motivated to postulate an initial period of expansion where the comoving Hubble horizon decreases, so that scales that are apparently out of causal contact now could have in fact communicated with one another early on. This conjecture, called Cosmological Inflation, dynamically explains most of the shortcomings of the Big Bang model and has received continuous observational support in the last decades. We then proceeded to discuss the transition from the inflationary period to the Hot Big Bang, the reheating stage. Although the details of this period are difficult to probe observationally, one can attempt to provide a macroscopic description, based on the reheating number of e-folds, which is related to the duration of inflation and to other benchmark epochs of cosmic evolution through the matching equation and its variations. At last, we focused on the current concordance model of Cosmology, the ΛCDM. It was formulated in the late 1990s and early 2000s, as the result of high-precision measurements that further supported the existence of cold dark matter and provided solid evidence for a dark energy component. Currently, this successful paradigm has been facing the observational challenge of reconciling independent measurements of some of its parameters, namely the Hubble constant H_0 and the clustering of matter σ_8.

In Chapter 2 we delved deeper into the realm of Particle Physics, in order to discuss some well established aspects of our inflaton candidate, the Higgs boson. First, we discussed the role of the Higgs in the Standard Model, primarily in the Higgs mechanism of electroweak symmetry breaking and generation of masses for fermions and massive gauge bosons. Then, we analysed a popular inflationary model of the late 2000s in which the Higgs is non-minimally coupled to gravity. We performed the slow-roll analysis of the Einstein frame potential and showed that it provides great agreement with latest CMB

data.

Finally, Chapter 3 is concerned with our work developed in [Rodrigues et al., 2023]. There, we extend the model of non-minimal Higgs inflation with the inclusion of radiative corrections. In order to account for quantum effects, we work with the one-loop effective potential, where the first corrections due to absorption and emission of virtual particles are included in the scalar field potential energy. We proceed with the usual treatment of non-minimal inflationary models, with the computation of slow-roll parameters in the Einstein frame. As an initial analysis, we checked that the potential satisfies the CMB requirements for the scalar spectral index n_S and tensor-to-scalar ratio r, for small ranges of the radiative parameter a' and $N_k = 50, 55, 60$. In order to more carefully assess the effects of varying the inflationary number of e-folds, we perform a cosmological MCMC analysis with a modified spectrum of primordial perturbations, where, instead of the usual parametrization in terms of A_S and n_S, we use directly the inflationary potential as an input, in order to solve the system of Boltzmann equations. This allows us to constrain the parameters of the potential, mainly, the radiative parameter a', for each N_k. Then, we focused on the reheating stage, in order to further constrain our proposed inflationary e-fold number interval. As expected for successful slow-roll inflation, the subsequent stages of evolution, during reheating, are dominated by a potential approximately quadratic and, afterwards, quartic in the scalar field, which reproduces a matter- and radiation-like dominated expansion, respectively. Thus, by relating the number of e-folds of inflation to the e-folds of reheating through the matching equation, we obtained an upper limit of $N_k \sim 56$, in order to have, at most, an instantaneous transition to the radiation-dominated epoch.

The main result of our work is twofold. First, we opted to develop a consistency check of the Higgs inflation scenario by relating our cosmological constraints on the radiative parameter a', to the electroweak scale, namely, by estimating the top quark mass. To this end, we solved the Renormalization Group Equations for different values of m_t, in order to obtain λ and β_λ near the Planck scale, which could be readily related to a'. For $N_k = 56$, we found $m_t \leqslant 170.44$ GeV. This estimate can be compared with the latest results from electroweak measurements. Assuming the analysis of $t\bar{t}$ events from the LHC and Tevatron team, one finds $m_t = 172.69 \pm 0.30$ GeV, representing a 7.5σ discrepancy with our result. Instead, one can consider the computation of the cross-section of top quark production, yielding $m_t = 172.5 \pm 0.7$ GeV from LHC and Tevatron runs - lowering the tension to $\approx 3\sigma$ - and $m_t = 170.5 \pm 0.8$ GeV from the CMS collaboration - which agrees with our cosmological estimation. Second, the MCMC analysis with current cosmological data reported a breaking of the $H_0 - \sigma_8$ correlation for the inflationary e-fold number larger than 54.5. For the instantaneous transition to the radiation-dominated epoch, which corresponds to fixing $N_k = 56$, the H_0 tension is slightly reduced to $\approx 3\sigma$, while the clustering parameter is constrained at $\sigma_8 = 0.793 \pm 0.003$, consistent with the

latest weak gravitational lensing measurements.

Therefore, based on the latest particle physics phenomenology results, one cannot completely rule out the Higgs inflation scenario, as new data from collider experiments are needed in order to better constrain this hypothesis. Also, the capability of the model to alleviate ongoing cosmological tensions makes it interesting from the observational point of view. We hope that novel theoretical and experimental insights in the fields of Cosmology and Particle Physics come to light in the near future, in an effort to better investigate the Higgs inflation conjecture and alternatives thereof.

Bibliography

Georges Aad et al. Observation of a new particle in the search for the Standard Model Higgs boson with the ATLAS detector at the LHC. *Phys. Lett.*, B716:1–29, 2012. doi: 10.1016/j.physletb.2012.08.020.

V. M. Abazov et al. A precision measurement of the mass of the top quark. *Nature*, 429: 638–642, 2004. doi: 10.1038/nature02589.

F. Abe et al. Evidence for top quark production in $\bar{p}p$ collisions at $\sqrt{s} = 1.8$ TeV. *Phys. Rev. D*, 50:2966–3026, 1994. doi: 10.1103/PhysRevD.50.2966.

P. A. R. Ade et al. BICEP2 / Keck Array x: Constraints on Primordial Gravitational Waves using Planck, WMAP, and New BICEP2/Keck Observations through the 2015 Season. *Phys. Rev. Lett.*, 121:221301, 2018. doi: 10.1103/PhysRevLett.121.221301.

N. Aghanim et al. Planck 2018 results. VI. Cosmological parameters. *Astron. Astrophys.*, 641:A6, 2020a. doi: 10.1051/0004-6361/201833910. [Erratum: Astron.Astrophys. 652, C4 (2021)].

N. Aghanim et al. Planck 2018 results. V. CMB power spectra and likelihoods. *Astron. Astrophys.*, 641:A5, 2020b. doi: 10.1051/0004-6361/201936386.

Y. Akrami et al. Planck 2018 results. X. Constraints on inflation. *Astron. Astrophys.*, 641:A10, 2020. doi: 10.1051/0004-6361/201833887.

Shadab Alam et al. The clustering of galaxies in the completed SDSS-III Baryon Oscillation Spectroscopic Survey: cosmological analysis of the DR12 galaxy sample. *Mon. Not. Roy. Astron. Soc.*, 470(3):2617–2652, 2017. doi: 10.1093/mnras/stx721.

Marika Asgari et al. KiDS-1000 Cosmology: Cosmic shear constraints and comparison between two point statistics. *Astron. Astrophys.*, 645:A104, 2021. doi: 10.1051/0004-6361/202039070.

J. L. F. Barbon and J. R. Espinosa. On the Naturalness of Higgs Inflation. *Phys. Rev.*, D79:081302, 2009. doi: 10.1103/PhysRevD.79.081302.

A. O. Barvinsky, A. Yu. Kamenshchik, and A. A. Starobinsky. Inflation scenario via the Standard Model Higgs boson and LHC. *JCAP*, 0811:021, 2008. doi: 10.1088/1475-7516/2008/11/021.

Daniel Baumann. Tasi lectures on inflation, 2012.

Daniel Baumann. *Cosmology*. Cambridge University Press, 7 2022. ISBN 978-1-108-93709-2, 978-1-108-83807-8. doi: 10.1017/9781108937092.

Florian Beutler, Chris Blake, Matthew Colless, D. Heath Jones, Lister Staveley-Smith, Lachlan Campbell, Quentin Parker, Will Saunders, and Fred Watson. The 6dF Galaxy Survey: Baryon Acoustic Oscillations and the Local Hubble Constant. *Mon. Not. Roy. Astron. Soc.*, 416:3017–3032, 2011. doi: 10.1111/j.1365-2966.2011.19250.x.

F. Bezrukov, D. Gorbunov, and M. Shaposhnikov. On initial conditions for the Hot Big Bang. *JCAP*, 0906:029, 2009. doi: 10.1088/1475-7516/2009/06/029.

Fedor L. Bezrukov and Mikhail Shaposhnikov. The Standard Model Higgs boson as the inflaton. *Phys. Lett.*, B659:703–706, 2008. doi: 10.1016/j.physletb.2007.11.072.

N. D. Birrell and P. C. W. Davies. *Quantum Fields in Curved Space*. Cambridge Monographs on Mathematical Physics. Cambridge Univ. Press, Cambridge, UK, 1984. ISBN 0521278589, 9780521278584, 9780521278584. doi: 10.1017/CBO9780511622632.

C. P. Burgess, Hyun Min Lee, and Michael Trott. Comment on Higgs Inflation and Naturalness. *JHEP*, 07:007, 2010. doi: 10.1007/JHEP07(2010)007.

Mathias Butenschoen, Bahman Dehnadi, André H. Hoang, Vicent Mateu, Moritz Preisser, and Iain W. Stewart. Top quark mass calibration for monte carlo event generators. *Phys. Rev. Lett.*, 117:232001, Nov 2016. doi: 10.1103/PhysRevLett.117.232001. URL https://link.aps.org/doi/10.1103/PhysRevLett.117.232001.

Dario Buttazzo, Giuseppe Degrassi, Pier Paolo Giardino, Gian F. Giudice, Filippo Sala, Alberto Salvio, and Alessandro Strumia. Investigating the near-criticality of the Higgs boson. *JHEP*, 12:089, 2013. doi: 10.1007/JHEP12(2013)089.

Serguei Chatrchyan et al. Observation of a New Boson at a Mass of 125 GeV with the CMS Experiment at the LHC. *Phys. Lett.*, B716:30–61, 2012. doi: 10.1016/j.physletb.2012.08.021.

Sidney R. Coleman and Erick J. Weinberg. Radiative Corrections as the Origin of Spontaneous Symmetry Breaking. *Phys. Rev.*, D7:1888–1910, 1973. doi: 10.1103/PhysRevD.7.1888.

Jessica L. Cook, Emanuela Dimastrogiovanni, Damien A. Easson, and Lawrence M. Krauss. Reheating predictions in single field inflation. *JCAP*, 04:047, 2015. doi: 10.1088/1475-7516/2015/04/047.

Eleonora Di Valentino, Olga Mena, Supriya Pan, Luca Visinelli, Weiqiang Yang, Alessandro Melchiorri, David F. Mota, Adam G. Riess, and Joseph Silk. In the realm of the Hubble tension—a review of solutions. *Class. Quant. Grav.*, 38(15):153001, 2021a. doi: 10.1088/1361-6382/ac086d.

Eleonora Di Valentino et al. Cosmology Intertwined III: $f\sigma_8$ and S_8. *Astropart. Phys.*, 131:102604, 2021b. doi: 10.1016/j.astropartphys.2021.102604.

Eleonora Di Valentino et al. Snowmass2021 - Letter of interest cosmology intertwined II: The hubble constant tension. *Astropart. Phys.*, 131:102605, 2021c. doi: 10.1016/j.astropartphys.2021.102605.

Scott Dodelson. *Modern Cosmology*. Academic Press, Amsterdam, 2003. ISBN 978-0-12-219141-1.

Albert Einstein. Zur Allgemeinen Relativitätstheorie. *Sitzungsber. Preuss. Akad. Wiss. Berlin (Math. Phys.)*, 1915:778–786, 1915. [Addendum: Sitzungsber.Preuss.Akad.Wiss.Berlin (Math.Phys.) 1915, 799–801 (1915)].

F. Englert and R. Brout. Broken symmetry and the mass of gauge vector mesons. *Phys. Rev. Lett.*, 13:321–323, Aug 1964. doi: 10.1103/PhysRevLett.13.321. URL https://link.aps.org/doi/10.1103/PhysRevLett.13.321.

Valerio Faraoni, Edgard Gunzig, and Pasquale Nardone. Conformal transformations in classical gravitational theories and in cosmology. *Fund. Cosmic Phys.*, 20:121, 1999.

R. P. Feynman and M. Gell-Mann. Theory of the fermi interaction. *Phys. Rev.*, 109:193–198, Jan 1958. doi: 10.1103/PhysRev.109.193. URL https://link.aps.org/doi/10.1103/PhysRev.109.193.

Alexander Alexandrovich Friedmann. On the curvature of space. *Z. Phys.*, 10:377–386, 1922. ISSN 0939-7922.

Juan Garcia-Bellido, Daniel G. Figueroa, and Javier Rubio. Preheating in the Standard Model with the Higgs-Inflaton coupled to gravity. *Phys. Rev.*, D79:063531, 2009. doi: 10.1103/PhysRevD.79.063531.

Sheldon L. Glashow. The renormalizability of vector meson interactions. *Nuclear Physics*, 10:107–117, 1959. ISSN 0029-5582. doi: https://doi.org/10.1016/0029-5582(59)90196-8. URL https://www.sciencedirect.com/science/article/pii/0029558259901968.

Jinn-Ouk Gong, Shi Pi, and Godfrey Leung. Probing reheating with primordial spectrum. *JCAP*, 05:027, 2015. doi: 10.1088/1475-7516/2015/05/027.

G. S. Guralnik, C. R. Hagen, and T. W. B. Kibble. Global conservation laws and massless particles. *Phys. Rev. Lett.*, 13:585–587, Nov 1964. doi: 10.1103/PhysRevLett.13.585. URL https://link.aps.org/doi/10.1103/PhysRevLett.13.585.

Alan H. Guth. The Inflationary Universe: A Possible Solution to the Horizon and Flatness Problems. *Phys. Rev.*, D23:347–356, 1981. doi: 10.1103/PhysRevD.23.347.

Stephen Hawking and W. Israel. *General Relativity: an Einstein Centenary Survey*. 2010.

Peter W. Higgs. Broken symmetries and the masses of gauge bosons. *Phys. Rev. Lett.*, 13:508–509, Oct 1964. doi: 10.1103/PhysRevLett.13.508. URL https://link.aps.org/doi/10.1103/PhysRevLett.13.508.

Edwin Hubble. A relation between distance and radial velocity among extra-galactic nebulae. *Proc. Nat. Acad. Sci.*, 15:168–173, 1929. doi: 10.1073/pnas.15.3.168.

Edwin Hubble. The Distribution of Extra-Galactic Nebulae. Astrophys. J., 79:8, January 1934. doi: 10.1086/143517.

Lev Kofman, Andrei D. Linde, and Alexei A. Starobinsky. Reheating after inflation. *Phys. Rev. Lett.*, 73:3195–3198, 1994. doi: 10.1103/PhysRevLett.73.3195.

Lev Kofman, Andrei D. Linde, and Alexei A. Starobinsky. Towards the theory of reheating after inflation. *Phys. Rev. D*, 56:3258–3295, 1997. doi: 10.1103/PhysRevD.56.3258.

U. Langenfeld, S. Moch, and P. Uwer. Measuring the running top-quark mass. *Phys. Rev. D*, 80:054009, 2009. doi: 10.1103/PhysRevD.80.054009.

Andrew R Liddle and Samuel M Leach. How long before the end of inflation were observable perturbations produced? *Phys. Rev.*, D68:103503, 2003. doi: 10.1103/PhysRevD.68.103503.

David H. Lyth and Andrew R. Liddle. *The primordial density perturbation: Cosmology, inflation and the origin of structure*. 2009.

Viatcheslav F Mukhanov and GV Chibisov. Quantum fluctuations and a nonsingular universe. *JETP Letters*, 33(10):532–535, 1981.

A. Pais. *INWARD BOUND OF MATTER AND FORCES IN THE PHYSICAL WORLD*. 1986.

P. Pascual and R. Tarrach. *QCD: RENORMALIZATION FOR THE PRACTITIONER*, volume 194. 1984.

P. J. E. Peebles. *Cosmology's Century: An Inside History of Our Modern Understanding of the Universe*. Princeton University Press, 2020. ISBN 978-0-691-19602-2.

Adam G. Riess et al. Observational evidence from supernovae for an accelerating universe and a cosmological constant. *Astron. J.*, 116:1009–1038, 1998. doi: 10.1086/300499.

Adam G. Riess et al. A Comprehensive Measurement of the Local Value of the Hubble Constant with 1 km s^1 Mpc^1 Uncertainty from the Hubble Space Telescope and the SH0ES Team. *Astrophys. J. Lett.*, 934(1):L7, 2022. doi: 10.3847/2041-8213/ac5c5b.

Jamerson G. Rodrigues, Micol Benetti, and Jailson S. Alcaniz. Possible discrepancies between cosmological and electroweak observables in Higgs Inflation. *JHEP*, 11:091, 2021. doi: 10.1007/JHEP11(2021)091.

Jamerson G. Rodrigues, Micol Benetti, Rayff de Souza, and Jailson Alcaniz. Higgs Inflation: constraining the top quark mass and breaking the H_0-σ_8 correlation. 1 2023.

Ashley J. Ross, Lado Samushia, Cullan Howlett, Will J. Percival, Angela Burden, and Marc Manera. The clustering of the SDSS DR7 main Galaxy sample I : A 4 per cent distance measure at $z = 0.15$. *Mon. Not. Roy. Astron. Soc.*, 449(1):835–847, 2015. doi: 10.1093/mnras/stv154.

Vera C. Rubin, W. Kent Ford, Jr., and Norbert Thonnard. Extended rotation curves of high-luminosity spiral galaxies. IV. Systematic dynamical properties, Sa through Sc. *Astrophys. J. Lett.*, 225:L107–L111, 1978. doi: 10.1086/182804.

Abdus Salam. Weak and Electromagnetic Interactions. *Conf. Proc. C*, 680519:367–377, 1968. doi: 10.1142/9789812795915_0034.

Matthew D. Schwartz. *Quantum Field Theory and the Standard Model*. Cambridge University Press, 3 2014. ISBN 978-1-107-03473-0, 978-1-107-03473-0.

D. M. Scolnic et al. The Complete Light-curve Sample of Spectroscopically Confirmed SNe Ia from Pan-STARRS1 and Cosmological Constraints from the Combined Pantheon Sample. *Astrophys. J.*, 859(2):101, 2018. doi: 10.3847/1538-4357/aab9bb.

Marc Sher. Electroweak Higgs Potentials and Vacuum Stability. *Phys. Rept.*, 179:273–418, 1989. doi: 10.1016/0370-1573(89)90061-6.

Albert M Sirunyan et al. Measurement of $t\bar{t}$ normalised multi-differential cross sections in pp collisions at $\sqrt{s} = 13$ TeV, and simultaneous determination of the strong coupling strength, top quark pole mass, and parton distribution functions. *Eur. Phys. J. C*, 80(7):658, 2020. doi: 10.1140/epjc/s10052-020-7917-7.

Alexei A. Starobinsky. A New Type of Isotropic Cosmological Models Without Singularity. *Phys. Lett.*, 91B:99–102, 1980. doi: 10.1016/0370-2693(80)90670-X. [,771(1980)].

Michael S. Turner. Coherent Scalar Field Oscillations in an Expanding Universe. *Phys. Rev. D*, 28:1243, 1983. doi: 10.1103/PhysRevD.28.1243.

L. Verde, T. Treu, and A. G. Riess. Tensions between the Early and the Late Universe. In *Nature Astronomy 2019*, 2019. doi: 10.1038/s41550-019-0902-0.

Steven Weinberg. A model of leptons. *Phys. Rev. Lett.*, 19:1264–1266, Nov 1967. doi: 10.1103/PhysRevLett.19.1264. URL https://link.aps.org/doi/10.1103/PhysRevLett.19.1264.

R. L. Workman and Others. Review of Particle Physics. *PTEP*, 2022:083C01, 2022. doi: 10.1093/ptep/ptac097.

C. S. Wu, E. Ambler, R. W. Hayward, D. D. Hoppes, and R. P. Hudson. Experimental test of parity conservation in beta decay. *Phys. Rev.*, 105:1413–1415, Feb 1957. doi: 10.1103/PhysRev.105.1413. URL https://link.aps.org/doi/10.1103/PhysRev.105.1413.

A. Zee. *Quantum field theory in a nutshell*. 2003. ISBN 978-0-691-14034-6.

F. Zwicky. Die Rotverschiebung von extragalaktischen Nebeln. *Helv. Phys. Acta*, 6:110–127, 1933. doi: 10.1007/s10714-008-0707-4.

P.A. Zyla et al. Review of Particle Physics. *PTEP*, 2020(8):083C01, 2020. doi: 10.1093/ptep/ptaa104.